U.S. Department of Transportation

Federal Railroad Administration

Low Solar Absorption Coating for Reducing Rail Temperature and Preventing Buckling

Office of Research,
Development
and Technology
Washington, DC 20590

DOT/FRA/ORD-18/28

Final Report
July 2018

REPORT DOCUMENTATION PAGE

Form Approved
OMB No. 0704-0188

1. AGENCY USE ONLY (Leave blank)	2. REPORT DATE	3. REPORT TYPE AND DATES COVERED
	July 2018	Technical Report August 2013–September 2015

4. TITLE AND SUBTITLE
Low Solar Absorption Coating for Reducing Rail Temperature and Preventing Buckling

5. FUNDING NUMBERS
DTFR53-13-C-00060

6. AUTHOR(S)
Dr. Hao Wang and Dr. Perumalsamy Balaguru

7. PERFORMING ORGANIZATION NAME(S) AND ADDRESS(ES)
Department of Civil and Environmental Engineering
Rutgers, The State University of New Jersey
96 Frelinghuysen Road
Piscataway, NJ 08854

8. PERFORMING ORGANIZATION REPORT NUMBER

9. SPONSORING/MONITORING AGENCY NAME(S) AND ADDRESS(ES)
U.S. Department of Transportation
Federal Railroad Administration
Office of Railroad Policy and Development
Office of Research, Development and Technology
Washington, DC 20590

10. SPONSORING/MONITORING AGENCY REPORT NUMBER
DOT/FRA/ORD-18/28

11. SUPPLEMENTARY NOTES
COR: Cameron D. Stuart

12a. DISTRIBUTION/AVAILABILITY STATEMENT
This document is available to the public through the FRA Web site at http://www.fra.dot.gov.

12b. DISTRIBUTION CODE

13. ABSTRACT (Maximum 200 words)
This report documents Rutgers University's research in the development and demonstration of an inorganic coating for reducing peak rail temperature to inhibit rail buckling. The zero-volatile organic content (VOC) and 100 percent inorganic coating system is based on an alkali-aluminosilicate composite formulation. The outdoor experimental results showed that the maximum temperature reduction provided by the coating was approximately 20 ºF. Field application of the coating was carried out on the actual track in Manville, NJ. It was discovered that the measurement of rail temperature is affected by the localized effect of rail surface with different solar absorption coefficients such as the metal attachment in the magnetic temperature sensor. Three-dimensional finite element models were developed to predict temperature distributions and thermal stresses in the rail. The coating application could reduce the high rail neutral temperature (RNT) requirement during rail placement and prevent rail buckling when the effective RNT decreased after traffic and maintenance. Field application of the coating demonstrated that it adheres well to the rails and has good durability. The coating can be applied using regular equipment such as brushes or rollers.

14. SUBJECT TERMS
Solar absorption, inorganic coating, rail temperature, thermal stress, track buckling, zero-volatile organic content, VOC, rail neutral temperature, RNT

15. NUMBER OF PAGES
64

16. PRICE CODE

17. SECURITY CLASSIFICATION OF REPORT	18. SECURITY CLASSIFICATION OF THIS PAGE	19. SECURITY CLASSIFICATION OF ABSTRACT	20. LIMITATION OF ABSTRACT
Unclassified	Unclassified	Unclassified	

NSN 7540-01-280-5500
Standard Form 298 (Rev. 2-89)
Prescribed by ANSI Std. 239-18
298-102

METRIC/ENGLISH CONVERSION FACTORS

ENGLISH TO METRIC

LENGTH (APPROXIMATE)

1 inch (in)	=	2.5 centimeters (cm)
1 foot (ft)	=	30 centimeters (cm)
1 yard (yd)	=	0.9 meter (m)
1 mile (mi)	=	1.6 kilometers (km)

AREA (APPROXIMATE)

1 square inch (sq in, in^2)	=	6.5 square centimeters (cm^2)
1 square foot (sq ft, ft^2)	=	0.09 square meter (m^2)
1 square yard (sq yd, yd^2)	=	0.8 square meter (m^2)
1 square mile (sq mi, mi^2)	=	2.6 square kilometers (km^2)
1 acre = 0.4 hectare (he)	=	4,000 square meters (m^2)

MASS - WEIGHT (APPROXIMATE)

1 ounce (oz)	=	28 grams (gm)
1 pound (lb)	=	0.45 kilogram (kg)
1 short ton = 2,000 pounds (lb)	=	0.9 tonne (t)

VOLUME (APPROXIMATE)

1 teaspoon (tsp)	=	5 milliliters (ml)
1 tablespoon (tbsp)	=	15 milliliters (ml)
1 fluid ounce (fl oz)	=	30 milliliters (ml)
1 cup (c)	=	0.24 liter (l)
1 pint (pt)	=	0.47 liter (l)
1 quart (qt)	=	0.96 liter (l)
1 gallon (gal)	=	3.8 liters (l)
1 cubic foot (cu ft, ft^3)	=	0.03 cubic meter (m^3)
1 cubic yard (cu yd, yd^3)	=	0.76 cubic meter (m^3)

TEMPERATURE (EXACT)

[(x-32)(5/9)] °F = y °C

METRIC TO ENGLISH

LENGTH (APPROXIMATE)

1 millimeter (mm)	=	0.04 inch (in)
1 centimeter (cm)	=	0.4 inch (in)
1 meter (m)	=	3.3 feet (ft)
1 meter (m)	=	1.1 yards (yd)
1 kilometer (km)	=	0.6 mile (mi)

AREA (APPROXIMATE)

1 square centimeter (cm^2)	=	0.16 square inch (sq in, in^2)
1 square meter (m^2)	=	1.2 square yards (sq yd, yd^2)
1 square kilometer (km^2)	=	0.4 square mile (sq mi, mi^2)
10,000 square meters (m^2)	=	1 hectare (ha) = 2.5 acres

MASS - WEIGHT (APPROXIMATE)

1 gram (gm)	=	0.036 ounce (oz)
1 kilogram (kg)	=	2.2 pounds (lb)
1 tonne (t)	=	1,000 kilograms (kg)
	=	1.1 short tons

VOLUME (APPROXIMATE)

1 milliliter (ml)	=	0.03 fluid ounce (fl oz)
1 liter (l)	=	2.1 pints (pt)
1 liter (l)	=	1.06 quarts (qt)
1 liter (l)	=	0.26 gallon (gal)
1 cubic meter (m^3)	=	36 cubic feet (cu ft, ft^3)
1 cubic meter (m^3)	=	1.3 cubic yards (cu yd, yd^3)

TEMPERATURE (EXACT)

[(9/5) y + 32] °C = x °F

QUICK INCH - CENTIMETER LENGTH CONVERSION

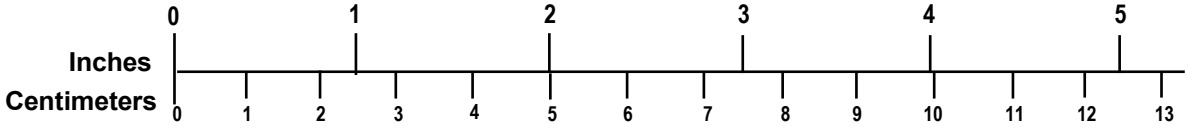

QUICK FAHRENHEIT - CELSIUS TEMPERATURE CONVERSIO

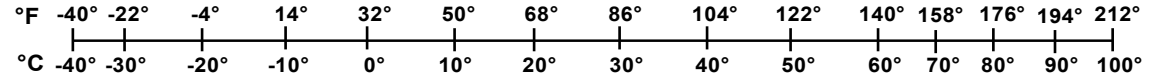

For more exact and or other conversion factors, see NIST Miscellaneous Publication 286, Units of Weights and Measures. Price $2.50 SD Catalog No. C13 10286

Updated 6/17/98

Acknowledgements

The authors would like to acknowledge and express their sincere thanks to Norfolk Southern Corporation for their cooperation during the field implementation. Special thanks to Mr. Brad Kerchof and Mr. Jason A. Trompeter as well.

Contents

Illustrations

Tables

Executive Summary

Rutgers University performed this research between August 2013 and September 2015 with funding by the Federal Railroad Administration to develop and demonstrate the use of an inorganic coating for reducing peak rail temperatures and preventing rail buckling. The zero-volatile organic content (VOC) and 100 percent inorganic coating system is based on an alkali-aluminosilicate composite formulation. The key characteristics of the coating are its low solar absorption properties and durability in field environments.

Experiments were conducted using coated and uncoated rails exposed to sunlight at various ambient temperatures to evaluate the effectiveness of the coating in reducing rail temperature. The outdoor lab experimental results showed that the average temperature reduction provided by the coating was 21 ºF and the maximum reduction was 26 ºF. The coated rail temperature did not exceed 11 ºF above the ambient temperature. On average, the coating could reduce the temperature gain by 66 percent in the tested rail segments.

Field application of the coating was carried out on Norfolk Southern Corporation's track in Manville, NJ. Unfortunately, the temperature measurements made using an automated system did not provide verifiable results. The effect of measurement method on rail temperature was investigated using different instrumentation types (magnet sensor, thermocouple, and automated Salient system) and modeling simulations. It was discovered that the measurement of rail temperature is affected by the localized change of solar absorption of rail surface that could be caused by the metal cover in the temperature sensor. Considering this effect, the rail temperatures measured with the automated system were corrected. The corrected temperature difference between the uncoated and coated rail in the field track was found to be around 20 ºF, which was consistent with the observation from the outdoor laboratory measurement using the wired thermocouples.

Three-dimensional finite element models were developed to predict temperature distributions and thermal stresses in the rail. The simulation shows that, when the rail neutral temperature (RNT) is low, the coating decreases the compressive thermal stresses up to about 50 percent during the hottest hours. Although increasing the RNT decreases compressive thermal stresses in the rail, it increases the risk of a rail break (pull apart). The coating application could reduce the high RNT requirement during rail placement and prevent rail buckling when the effective RNT decreases after traffic and maintenance. Therefore, the low solar absorption coating could serve as a proactive way to control peak temperatures and thermal stresses in the rail.

The performance of the coated rail segments placed in the outdoor environment and the coated track in service were used to evaluate the durability of coating. Field application demonstrated that the coating adheres well to the rails. Extensive surface preparation is not needed and pressure washing with water is sufficient. Coating can be applied using regular equipment such as brushes or rollers. The curing time for allowing rail-traffic is about an hour. The coating can be applied on active tracks with proper scheduling. The durability of the coating was observed over summer and winter seasons and the coating performed well.

1. Introduction

This report documents research performed by Rutgers University between August 2013 and September 2015 and sponsored by the Federal Railroad Administration (FRA), to investigate the efficacy of inorganic coatings to reduce rail temperature rise due to solar absorption. The premise on which this research was based will be presented, as well as results from the development and demonstration of an inorganic coating for reducing peak rail temperatures and preventing rail buckling.

1.1 Background

In the natural environment, the temperature of structures continuously changes in response to climate. When restrained by boundary conditions, a thermal stress is created in the structure. For railway track, which is a long linear structure, thermal stresses due to temperature increase may become very significant during hot seasons. This increases the risk of track buckling caused derailments. According to statistical data from FRA's Office of Safety Analysis, within the year of 2012, at least 240 derailments happened throughout the United States, accounting for 79.5 percent of total train accidents [1]. Rail buckling due to excessive rail temperature is a major cause of these derailments [2] [3] [4] [5].

The most common technique employed by railroads to reduce the risk of derailments in hot seasons is speed reductions in response to increasing rail temperature. Although speed management is effective in prevention of derailment, it disrupts normal rail operation and causes costly delays [6]. In addition, such actions depend on the accuracy of rail temperature predictions [7]. Although several models have been developed to predict rail temperature based on weather data [8] [9], it is still difficult to prove that the prediction model is applicable for all weather conditions.

Reducing peak rail temperatures is a more proactive method to prevent track buckling. Low solar absorption coating technology has been one of the most effective ways to reduce pavement and roof temperatures. Solar reflectance is largely governed by color, and white color has better solar reflective properties than other colors. It was found that the reflectance decreases with the color changing from light to dark and it is also affected by surface roughness [10] [11] [12].

The coating system under test can be a near-white color providing the lowest solar absorption and thus considerably reducing the detrimental effects of heating and expansion of rails. The zero-volatile organic content (VOC) and one hundred percent inorganic coating system has constituents to provide very high abrasion resistance, self-cleaning properties, and excellent adhesion to steel surfaces with minimal surface preparation. The system is conducive for common application techniques such as spraying or application using brushes and rollers. The coating can also provide some protection against corrosion of rails exposed to salt environments.

1.2 Objectives

The objective of this study was to develop and demonstrate the field use of a low solar absorption coating for rail temperature reduction.

1.3 Overall Approach

The research approach includes coating material development, performance evaluation, numerical simulation, and field demonstration.

An inorganic composite coating was developed based on an alkali-aluminosilicate composite formulation. The key features of this coating are low solar absorption property and durability in field environments. Rail segments were coated for initial evaluation in the laboratory to provide information for surface preparation and coating application method.

The effectiveness of the coating for reducing solar-heat absorption was evaluated in the outdoor environment through temperature monitoring of rail segments with and without the coating in hot weather conditions. A three-dimensional (3D) finite element (FE) model was developed to simulate temperature profiles of the tested rail segments and predict thermal stresses in railway track under different rail surface conditions (coated vs. uncoated).

Researchers completed field tests of the coating on revenue service track in Manville, NJ. The test was coordinated by Norfolk Southern Corporation (NS). The tracks were instrumented to measure the temperatures and the effect of instrumentation on temperature measurement error was investigated. Coating performance and durability were evaluated in an outdoor lab environment and in revenue service track.

1.4 Scope

Major tasks of the research were:

- Development of a low solar absorption coating system
- Evaluation of coating performance for rail temperature reduction
- Demonstration of coating application and durability of coating under field conditions
- Preparation of guidelines for field applications

The outcome of this project is an efficient, environmental friendly, durable and economical coating system that can reduce peak temperature of rails. The performance of the coated rail is reported in terms of rail temperature reduction, durability, and application procedure.

1.5 Organization of Report

This report provides a comprehensive review of all project activities, conclusions, and future research recommendations. The report is organized into the following sections:

Section 1: Introduction

Section 2: Problem Description and Prior Work

Section 3: Development of Coating and Initial Laboratory Experiments

Section 4: Outdoor Laboratory Temperature Measurement

Section 5: Field Testing and Temperature Measurements

Section 6: Effects of Measurement Method on Rail Temperature

2. Problem Description and Prior Work

Railway tracks are constructed of four basic components: rails, ties, fasteners, and ballast. Steel rails are placed above the ties. Ties are typically constructed of wood or concrete, and serve to hold the rails upright and keep the correct gauge. Fasteners connect the rails to the ties. Ballast is gravel that serves as the top layer of grade material above the subgrade. The ballast serves to resist deforming forces in both the vertical and lateral (perpendicular to the rail) directions. Shoulder ballast can be effective in providing lateral restraint against rail buckling.

The component of primary concern for this project is the steel rail. Steel expands when heated and contracts as it cools. When connected as a track, rail sections are forced into compression when heated. The ultimate result may be buckling, typically in the lateral direction. This buckling can have several consequences. Trains must often reduce their speed for safety reasons due to the risk of derailment, resulting in delays. In 2012, record heat was blamed for a fatal train derailment in Northbrook, IL, killing two civilians travelling under the bridge where the train derailed [13].

Several methods have been used to prevent rail buckling, including pre-stressing of rails, expansion joints, train speed restrictions, and regular rail maintenance. Reducing rail peak temperature is a more proactive method to prevent derailments caused by thermal buckling. It is reported that solar absorptivity has significant positive effects on the maximum temperature, and low absorptivity material has been used in roadways to decrease pavement temperatures [14]. However, research on lowering solar absorption of rail is limited.

An important concept related to track buckling is the neutral, or stress free, rail temperature. Typically, rails are anchored at higher temperatures (35 to 43 °C) to induce tensile stresses that prevent compression-stress buckling at higher temperatures [15]. This is a form of pre-stressing can be an effective buckling restraint. However, in older rails, where such countermeasures have not been implemented, or wear and fatigue has set in by use, or maintenance has been neglected, this pre-stress may be reduced or lost entirely. A previous study sponsored by FRA concluded there are three major factors affecting rail buckling risk: high compressive forces, weakened track conditions, and vehicle loads [16].

2.1 Coatings to Reduce Solar-Heating

Coatings or paints have been developed to reflect sunlight and reduce heating for various types of applications including pavements and roofs. Most coatings are based on paints with filler additives. Ceramic-like coatings were found to be effective for reflecting near-infrared light [17]. Such coatings have been used for spacecraft, satellites and re-entry vehicles.

Two of the commonly used paints for metals are water based acrylic paints and epoxy based paints. Although it is debatable, in general, acrylic based paints are cheaper, inflexible (prone to cracking and peeling when material is deformed), and have poor corrosion protection properties. Epoxy based paints bond especially well to metals and have excellent corrosion properties. Epoxy paints are more expensive and tend to decompose or chalk when exposed to sunlight (ultraviolet light) [18]. However, the benefits and detractors of each type relative to each other

have been disputed by various sources. Typical commercial products used for many industrial and residential applications are water based acrylic paints.

Additives are commonly used to increase the coating's reflectance. Solacoat, which was the company found to market its product specifically for temperature reduction, uses a unique membrane added to water based acrylic paint, which reflects up to 82 percent of the suns solar rays [19]. Specifics on this additive were not provided by Solacoat. In other studies conducted on paint reflectance for buildings and conveyances, paints with ceramic additives were common [20]. One study specified using an epoxy based paint that had ceramic additives including Bionic Bubbles (derived from fly ash) and Insuladd particles (hollow ceramic microspheres). Paint with nano-additives was found to be more effective than regular paint in temperature reduction [21].

It was generally observed that white is the most favorable paint color for optimal temperature reduction. In addition, paint typically adheres to the metal surface better if a primer is applied beforehand. The primer used is typically specific to the type of paint. For example, a primer used in preparation for epoxy based paint will be epoxy based.

2.2 Coatings to Reduce Solar-Heating Specifically for Rails

Even though reflective coating is an effective way to reduce rail temperature, research in this area is limited. The Federal Transit Administration (FTA) has used reflective paint on mass transit rail cars to reduce interior heat for passengers. The concept of rail coating has been implemented in Australia, India, and the United Kingdom. In the United Kingdom, several stretches of Network Rail, the largest rail infrastructure in the country, have been painted white to counteract weather-caused rail buckling and train delays [22].

In 2005, Pacific Edge Pty, Ltd was requested by RailCorp (RIC) to arrange painting of rails (5 km of track) on the Carlingford Line between Camelia and Carlingford stations in Sydney, Australia. The Directors of Pacific Edge initiated Rail Painting in New South Wales whilst employed by the NSW Rail Industry. As a result, a private contractor (Pacific Edge) applied reflective paint coating to several kilometers of track at a location on the Carlingford Rail Line. In one location, 5 km of rail was painted with 1,500 liters of paint and anti-rust primer, as shown in Figure 1.

Figure 1. Coated Rails Near Sydney in Australia [19]

Temperature was logged continuously over a 5-day span on both coated and non-coated sections of the rail. Figure 2 shows the variation of ambient, coated and uncoated rail temperatures over a period of 5 days. The ambient temperature was approximately 30 to 37 °C for the test period. The non-coated section peaked at a temperature of 53 to 55 °C and the coated section peaked at a temperature of 43 to 48 °C. If the stress-free temperature of the rails was 35 °C, then the compressive stress due to temperature increase is approximately halved by coating according to Pacific Edge [23].

The experience showed a significant reduction in rail temperature, and rail painting is now an approved risk mitigation process against heat buckling in the NSW Rail Corp Civil Technical Notes, (Addendum to Standards). Based on this success, approximately 100 km were painted on the New South Wales North Coast Railway Line in 2002 and 2003. Other observations made during this application were: (1) thermal contact paste should be applied to the rail thermometer if field measurements are to be taken; and (2) rusty rail tends to show a lower temperature reading without such paste.

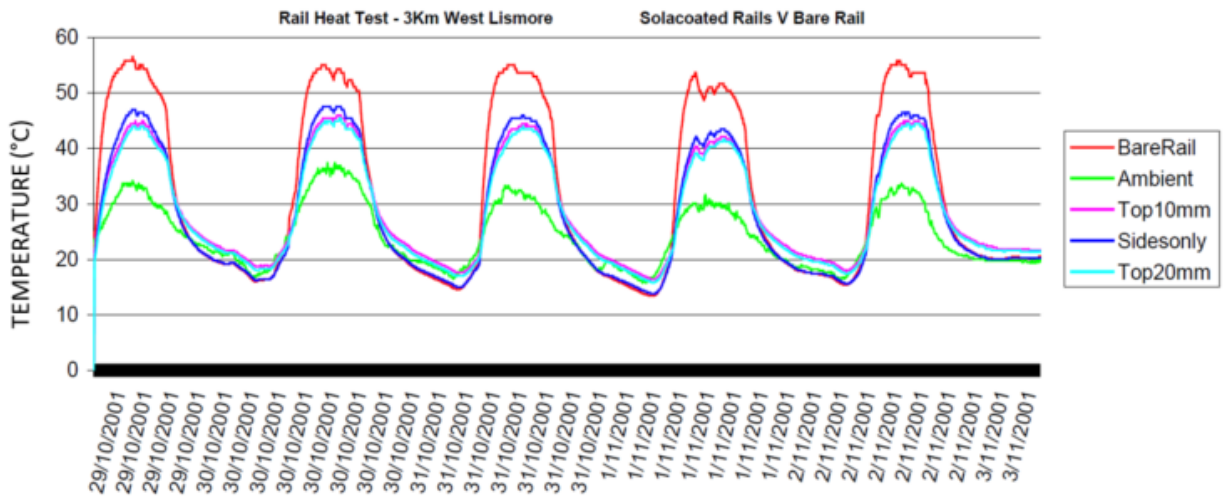

Figure 2. Variation of Ambient, Coated, and Uncoated Rails: Active Track in Australia [19]

A recent investigation conducted under the sponsorship of FRA and reported in a paper authored by Ritter and Al-Nazer is very closely related to the current investigation [24]. Therefore, the results reported in that paper are reviewed in detail. The study had two major tasks. In the first task several commercial coatings and additives were investigated for their potential to reduce heat gain on steel. Based on the results of this task, nine coatings were chosen for further evaluation. In the second task, rail segments were coated, instrumented with thermocouples, and placed outdoors in Ohio, for continuous exposure. Temperature data were recorded and analyzed for comparative performance ratings of the coatings, as shown in Figure 3.

For the second task, seven organic and three inorganic systems were chosen. Among the three inorganic systems only one was completely inorganic and it was based on a reactive phosphate system. This system is designated as Inorganic-1. The other two feature high levels of titanium oxide (Inorganic-2) or silica (Inorganic-3) fillers in a polymeric binder. The Inorganic 3 was discontinued due to poor bonding.

Table 1 summarizes the data obtained from the study. The study concluded that the inorganic coatings showed considerably better thermal performance than the organic coatings. Even though most of the coatings, whether organic or inorganic, provided enough performance to keep the temperature increase below 30 ºF, only the inorganic coating and possibly Rooftop-2 (2-coats) reduced the peak temperature by 10 ºF, as compared with uncoated steel. The inorganic coatings had a better potential to meet both performance criteria in thermal performance and durability.

Figure 3. Coated Rails Exposed to Sunlight [20]

Table 1. Temperature Reductions for Different Coatings on Bare and Rusted Steel [24]

Coating Type	Temperature Reduction (°F)	Maximum Gain (°F)
Inorganic-2	-14.2	18
Inorganic-1	-9.9	19.1
Rooftop-2, 2 coats	-9.2	26.1
Rooftop-1	-7.4	28.4
Rooftop-2, 1-coat	-7	27.2
Exterior latex – tan	-5.9	26.6
Exterior latex - tan with double micro-balloons	-5.4	28.8
Exterior latex tan - with micro-balloons	-5	27
Exterior latex - gray with micro-balloons	0.2	35.5
Bare Steel (control)	0	33.7
Rusty Steel	0	33.7

2.3 Summary

In summary, the following observations can be made based on the limited number of studies carried out for using reflective coating to improve performance of rails during the hot weather:

- Use of reflective coating is a viable option for reducing the buckling risk of rails during hot weather. Coatings can be successfully applied in the field, as demonstrated by the Australian team.
- Better performance provided by inorganic coatings can reduce rail temperature under solar heating.
- Small amounts of dirt on coatings do not reduce the performance of the coatings.
- It is possible to achieve temperature reduction of 10 ºF, and also limit the solar gain of temperature within 30 ºF by coating.

3. Development of Coating and Initial Laboratory Experiments

This section provides a synopsis of prior work completed to develop the specialized coating and detailed laboratory experiments to test the effectiveness of this coating for rail solar absorption

3.1 Development of Coating Formulation

The composite coating formulations were developed using an inorganic polymer from a previous study [25]. The earlier study resulted in the development of an alkali-aluminosilicate system that can be used for high strength composites using various high strength fibers including carbon fibers [26] [27]. The composition was enhanced with fillers for use in civil engineering structures for repair and rehabilitation. The primary requirements for the coatings were durability, abrasion resistance, self-cleaning and de-polluting properties and graffiti resistance [28].

Several field demonstration applications were carried out in early studies. The durability of coating system on concrete was successfully tested under 100 cycles of wetting-drying and 50 cycles of freezing-thawing. There was no degradation of the coating or the interface. The oldest coated surface was performing well after 20 years in service [29]. The maintenance crew could apply the coating with minimum training. This composition is more economical than most other coatings and used in several field-demonstration applications on concrete surfaces.

The coating formulation used in this study is potassium alumina-silicate, or poly sialate-siloxo with the general chemical structure:

$$K_n\{\text{-}(\ SiO_2)_z\text{-}\ AlO_{2}\text{-}\}_n \bullet wH_2O$$

Where, $z >> n$ and n is the degree of polycondensation; z is 1, 2, and 3; and w is the binding water amount. Features include:

- The resin is prepared by mixing a liquid component with a potassium-poly (sialate-siloxo) powder to a plastic consistency with the resulting mixture referred to as a matrix. Fillers and hardening agents can be added to the powder component to enhance the matrix properties.
- The matrix is water-based, consequently, tools and spills can be cleaned with water. All the components are nontoxic and no fumes are emitted during mixing or curing.
- Common application procedures are compatible with the matrix such as brushing, rolling and spraying.
- The base coating material is white, thus other color schemes can easily be formulated using pigments.
- The system is compatible with brick, concrete, wood, and steel.
- Zinc-oxide filler provides self-cleaning and de-polluting properties.
- The composition of coating contained the titanium oxide for achieving the maximum heat reflection.

In applications where the coated elements are subjected to severe environments, the inorganic system is expected to have a considerable advantage over the organic systems. The organic coatings could potentially soften at temperatures as low as 120 ºF and rail temperature could reach this temperature in summer periods. The softening and the follow-up hardening as the temperature goes down is a primary contributor to coating degradation. The organic coating also tends to delaminate with the formation of mud cracking after a few years. The proposed coating showed no delamination in concrete, steel, and timber surfaces. This was true even when high strains were induced by applying loading to the coated structural elements including steel beams.

The primary characteristics for the new coating development are low solar absorption property and durability in field environments. The outcome is an efficient, environmental friendly, durable and economical coating system that can reduce peak temperature of rails with the following features:

- The coating can be in near-white color providing least solar absorption.
- To enhance solar reflection at the infrared region, titanium dioxide is added.
- The coating will provide protection against corrosion where the rails are exposed to chemicals that cause corrosion.
- The constituents provide high abrasion resistance and hence damage due to occasional impact of stone-aggregates and blowing sand is avoided.
- The coating will not undergo any change up to temperature of 800 ºF. Organic coatings could soften at temperatures less than 150 ºF.
- Self-cleaning properties will prevent any organic growth in high humidity areas. Oil spills and dirt will not stick to the coating and therefore the brightness of the white color can be maintained for longer periods.

3.2 Indoor Temperature Measurement

The purpose of the initial experiment was to determine the effectiveness of the custom developed coating to reduce temperature gain when exposed to heat. Short rail segments were prepared after cutting one rail located at the Rutgers campus. The web and bottom flange of short rail sections were coated to simulate the actual field application. For the first run of this experiment, three pieces of rail were painted with different coating configurations and the test results were compared against each other. The configurations were 1) primed and painted on both sides, 2) primed and painted on one side and only primed on another side, 3) unpainted, as shown in Figure 4.

The initial experiment took place indoors using solar simulator lamps. The solar simulation was designed to reproduce the majority of heat energy transmitted through sunlight.

Rutgers selected the Infrared Heat Lamp (150 W) and the PowerSun UV Lamp (150 W) from ZooMed for heating sources. The PowerSun UV lamp covers the whole visible spectrum, plus UVA and UVB, while the Infrared Heat Lamp covers the radiation in the infrared range. Two identical apparatus setups included one infrared and one UV lamp inserted into a manufacturer designed Combo Deep Dome Lamp fixture. The fixtures were attached to the long table and the

painted and unpainted rail samples were set up underneath, as shown in Figure 5. K-type magnetic thermocouples from Omega were used to measure rail temperature. A commercial adhesive foam product was placed on the saw cut cross section portion of the rails for heat insulation. The foam used was Rubber Foam Weatherseal from Frost King.

Figure 4. Uncoated and Coated Short Rail Segments

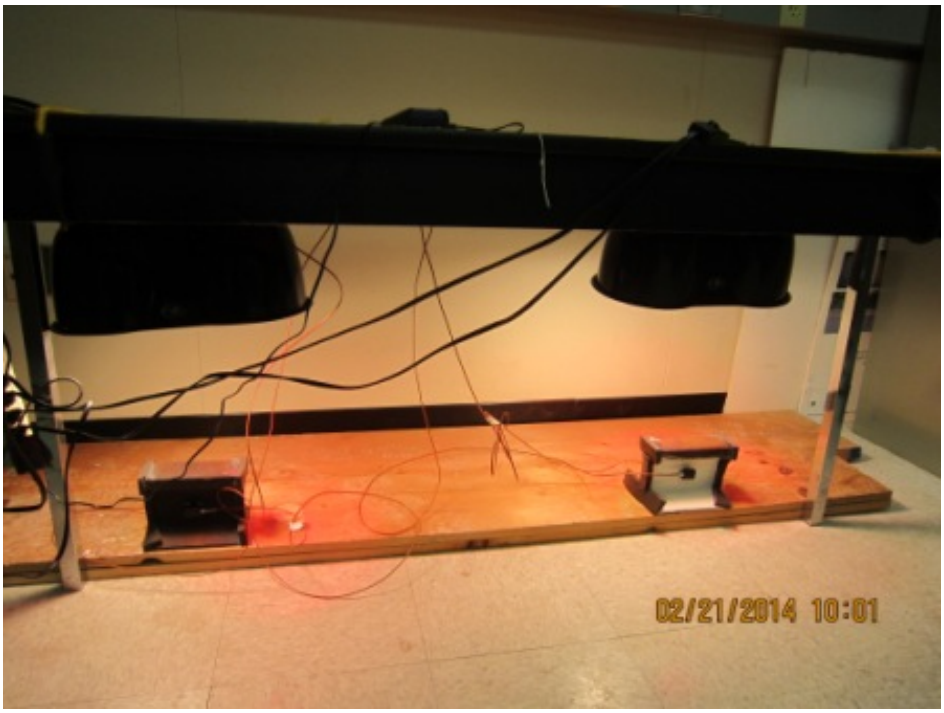

Figure 5. Short Rail Segments Exposed to Solar Lamps

Figure 6 shows the initial temperature measurements at different locations of the coated and uncoated rail samples when the solar lamp faced the rail at different angles. The results show that the coating reduced the surface temperature of the rails and it is most effective in the area where applied. It is noted that the temperature reduction at the web of the rail sample varies from 7–15 ºF under different testing conditions. This is probably because the solar energy emitted by the lamp is affected by the angle of lamp light with respect to the rail.

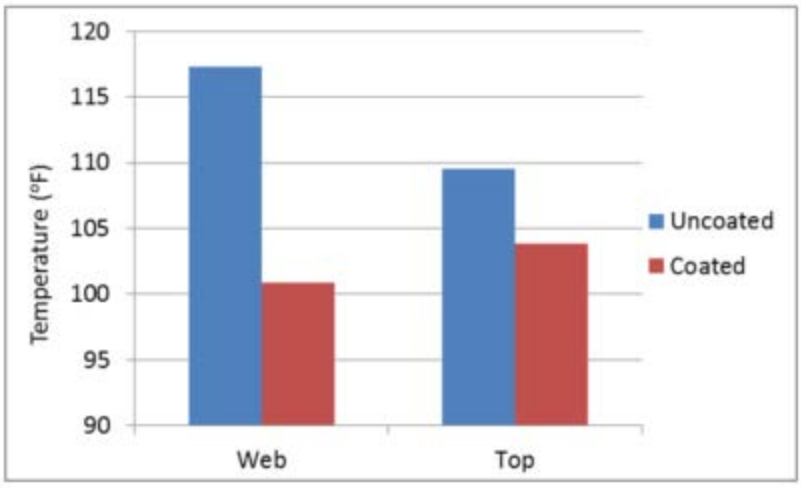

(a)

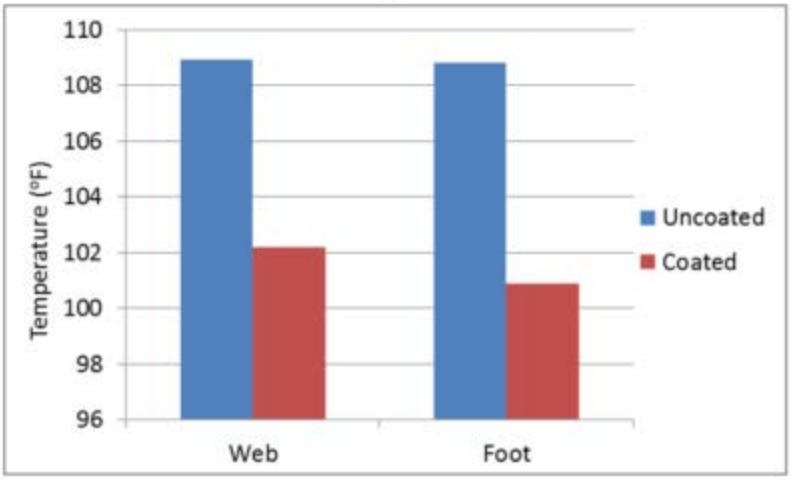

(b)

Figure 6. Temperature Measurements When Lamp is (a) Directly on Top of Rail and (b) Facing Rail with an Angle

4. Outdoor Laboratory Temperature Measurement

This section details the controlled outdoor experiments conducted to test the effectiveness of the rail coating.

4.1 Experimental Set-up

The 3-foot rail samples were obtained from the Pennsylvania Yard of NS. The samples were cleaning to remove hardened deposits, oil and loose rust. Then a first coat was applied as primer using rollers. After the first coat dried for a day, the second white coat was applied, as shown in Figure 7.

Figure 7. Coating on a 3-Foot Rail Segment

Outdoor experiments were conducted in the open area of Rutgers campus to measure the temperature of 3-foot rail segments with and without the coating in hot summer weather conditions. One coated and one uncoated rail segments were used in the experiment. The ends were protected by Styrofoam to simulate field conditions of actual rails.

We discovered that the magnets used to attach the thermocouples to the rail were affecting the temperature reading due to the magnet heating. The thermocouples were changed to wire thermocouples attached using thermal glue. Thermocouples were installed at the web and flange and connected to an Omega data logger set to record data every 60 seconds. Care was taken to make sure the set-up did not interfere with the measurement of rail temperature. A Vantage Pro2 weather station was used to measure the solar radiation, wind speed, humidity, and air temperature. The weather data was recorded automatically every 5 minutes. The experiment setup is shown in Figure 8.

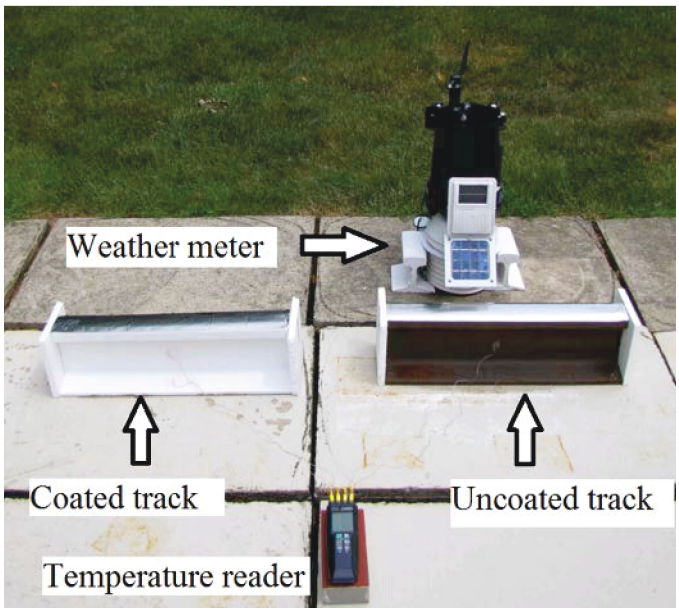

Figure 8. Experiment Setup of Outdoor Experiment

4.2 Temperature Measurement Results

The experiment was conducted on days when it was sunny and hot through June to August in 2014. The temperature data were collected through this period. Figure 9 to Figure 11 show the examples of recorded data for the ambient, uncoated and coated rail temperatures over 6, 24, 72-hour periods.

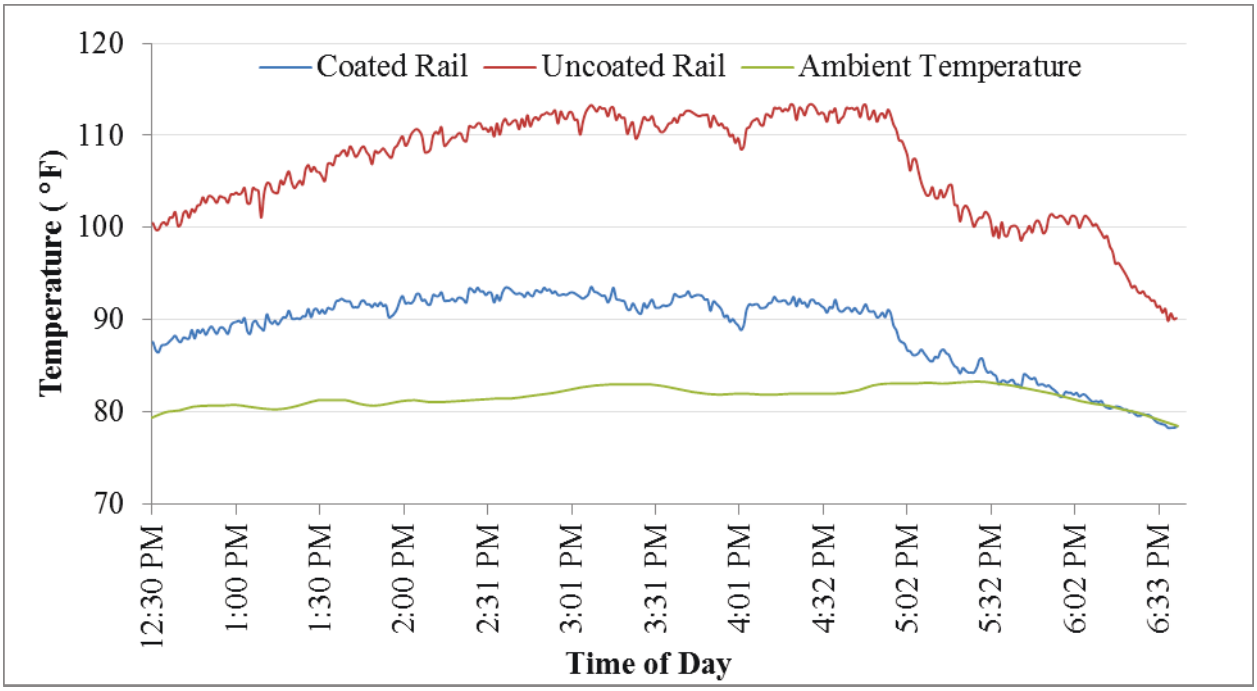

Figure 9. Example of Temperature Data from Outdoor Experiment for 6 Hours

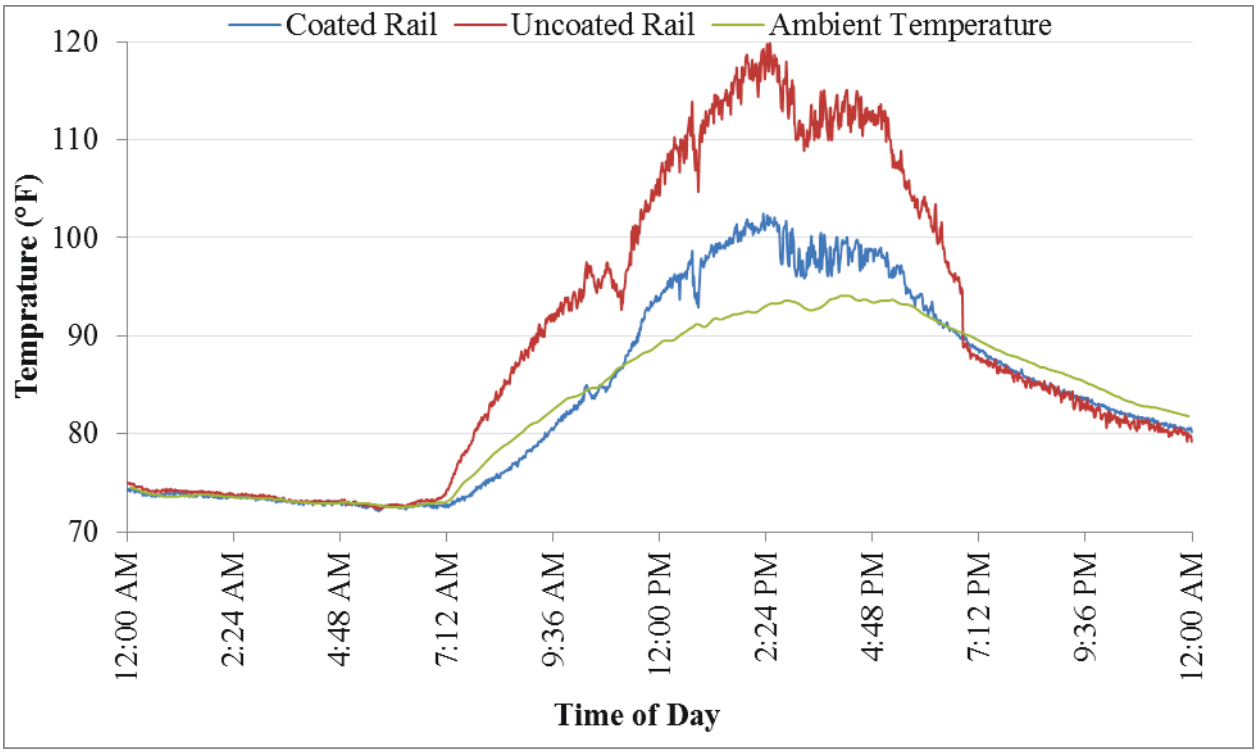

Figure 10. Example of Temperature Data from Outdoor Experiment for 24 Hours

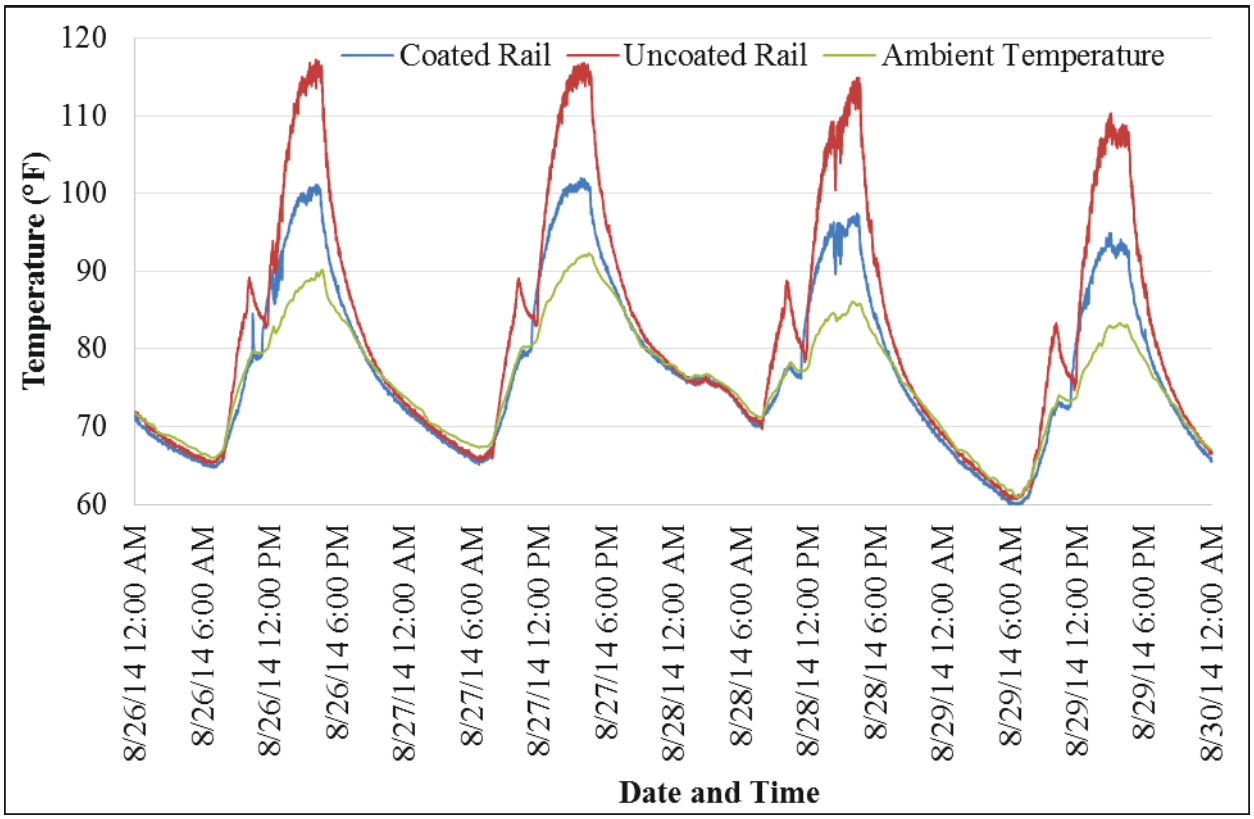

Figure 11. Example of Temperature Data from Outdoor Experiment for 72 Hours

The temperature data are summarized in Table 2. A careful analysis of the data and the figures lead to the following observations:

- The temperature reduction provided by the coating was 18–26 ºF.
- The coated rail temperature did not exceed 11 ºF above the ambient temperature for all cases.
- The coating could reduce the temperature gain by an average of 66 percent compared to the temperature of uncoated rail.
- For conditions in New Jersey, the peak temperature of the uncoated rail was around 25–33 ºF above the peak ambient temperatures with an average of 29 ºF.
- The results were consistent during the measuring period across several months.

Table 2. Summary of Temperature Results from Outdoor Experiments

Date	Monitoring Period (hour)	Peak ambient temperature (°F)	Peak temperature of uncoated rail (°F)	Peak temperature of coated rail (°F)	Temperature reduction due to coating (°F)
6/1/2014	6	83.3	113.4	93.6	22.1
6/2/2014	6	86.4	114.5	95.3	20.5
6/17/2014	7	92.5	120.5	103.4	18.3
6/18/2014	7	96.2	125.7	106.9	20.0
6/20/2014	6	86.6	118.9	95.7	24.0
6/28/2014	7	92.5	125.3	99.7	26.5
7/6/2014	7	91.2	120.4	99.5	21.6
7/7/2014	24	94.1	119.9	102.5	17.8
7/17/2014	24	88.5	117	99.6	20.1
8/7-8/9/2014	72	86.8	114.7	98.8	20.3
8/26-8/29/2014	72	92.3	117.2	102	20.3
Average		90.0	118.9	99.7	21.0

The findings presented here are consistent with the data reported in the recent study by Ritter and Al-Nazer [24]. In that study, the inorganic coating system had temperature reduction of 9.9 ºF and maximum temperature gain of 9.9 ºF, while the coating with a high amount of silica had temperature reduction of 14.0ºF and maximum temperature gain of 18.0 ºF. The coating used in the current investigation is totally inorganic and also has silica. Note that the measurements conducted in this study were made on similar rail segments and climate conditions as compared to the study at Ohio [20].

5. Field Testing and Temperature Measurements

This section details the field testing conducted by researchers at Rutgers. Pennsylvania State University supported testing at the Altoona, PA, site, and NS provided support for the testing on its in-service tracks.

5.1 Altoona Site

In addition to laboratory measurement of rail temperature conducted indoor and outdoor, field application of coating was conducted on the track at two different locations. In the first field application, conducted in April 2014, the coating was applied on rails located in the rail museum owned by Pennsylvania State University, Altoona College.

The effect of surface preparation on durability of coating was investigated. All rail surfaces were power-washed with water to remove oil, dirt, and loose corrosion. Additionally, one section of the rail had all corrosion removed by using grinding wheels. This process exposed the clean steel. All of these sections were first painted with the red metallic primer coating using paint rollers, (Figure 12). The primer was then allowed to cure overnight before the application of the white topcoat, shown in Figure 13. The surfaces on these rails were then protected from rainwater using poly-ethylene sheets in the first 24 hours after coating application. It is noted that the coating material has no toxic components and therefore there it is not a concern if the stone-aggregate base or sleepers are accidently coated in future large scale field applications.

The purpose of first field test is to evaluate if the coating durability is affected by the preparation of the existing rail surface. The performance evaluation consisted of visual inspection for any deterioration on the surface or interface of coated rail and the performance as a self-cleaning coating. This evaluation showed that the surface prepared with grinding had the same durability as the surface where rust remained.

Figure 12. Red Metallic Primer Coating

Figure 13. White Reflective Coating

5.2 Norfolk Southern Site

The second field application was conducted in May 2015 to evaluate coating performance in real world conditions and measure the rail temperature. The test site was Milepost LE 39.5, roughly 200 feet east of Royce Rd crossing in Manville, NJ, on NS.

The research team performed the coating installation under supervision. NS provided personnel to help in this application by stopping rail traffic to allow for surface application and to ensure safety.

Surface preparation was the first step in installation of the coating. An outside firm specializing in power-washing prepared two 15-foot sections of rail, using high-pressure water and an oil removing soapy solution. After rails were washed, researched allowed the surfaces to dry for 1 hour before coating was applied. Then the rails were coated with the red metallic primer using paint rollers, and allowed to cure overnight. The white top coat was then applied the next day using paint rollers. An area of the test rail was left uncoated to permit installation of the temperature monitors manufactured by L.B. Foster Salient Systems. Three temperature monitors were installed directly to rail surfaces, two on coated rail and one on uncoated rail. Temperature data were collected using a handheld wireless data collection device. Figure 14 to Figure 23 depict the process of coating application and installation of temperature monitor from Salient System.

After coating was installed, the rails experienced a light rain shower. Rails were observed later to see how coating was performing. Figure 24 shows the appearance of coating later after installation.

Figure 14. Surface Preparations Before Coating Using High Pressure Power Washing

Figure 15. Preparation of Red Metallic Primer Coating Mixture

Figure 16. Application of Red Metallic Primer to Rail with Roller

Figure 17. Dried Red Metallic Primer Coating on Rail

Figure 18. Preparation of White Surface Coating

Figure 19. Applying White Coating on Red Metallic Primer (the Patch Area for Installation of the Sensor is Covered with Blue Painter's Tape)

Figure 20. Sensor Installation on Rail with Coting

Figure 21. Completed Coating Application and Sensor Installation on Rail

Figure 22. Sensor Installation on Rail with Coting Without Coating

Figure 23. Completed Sensor Installation on Rail Without Coating

Figure 24. Rail After Light Rain Shower

5.3 Temperature Measurement Results

The automated temperature monitor provided continuous measurement of rail temperature at the NS site. The ambient temperatures were obtained from the public weather station close to the rail location. Figure 25 and Figure 26 show examples of temperature measurement data, respectively, for the air, coated rail, and uncoated rail.

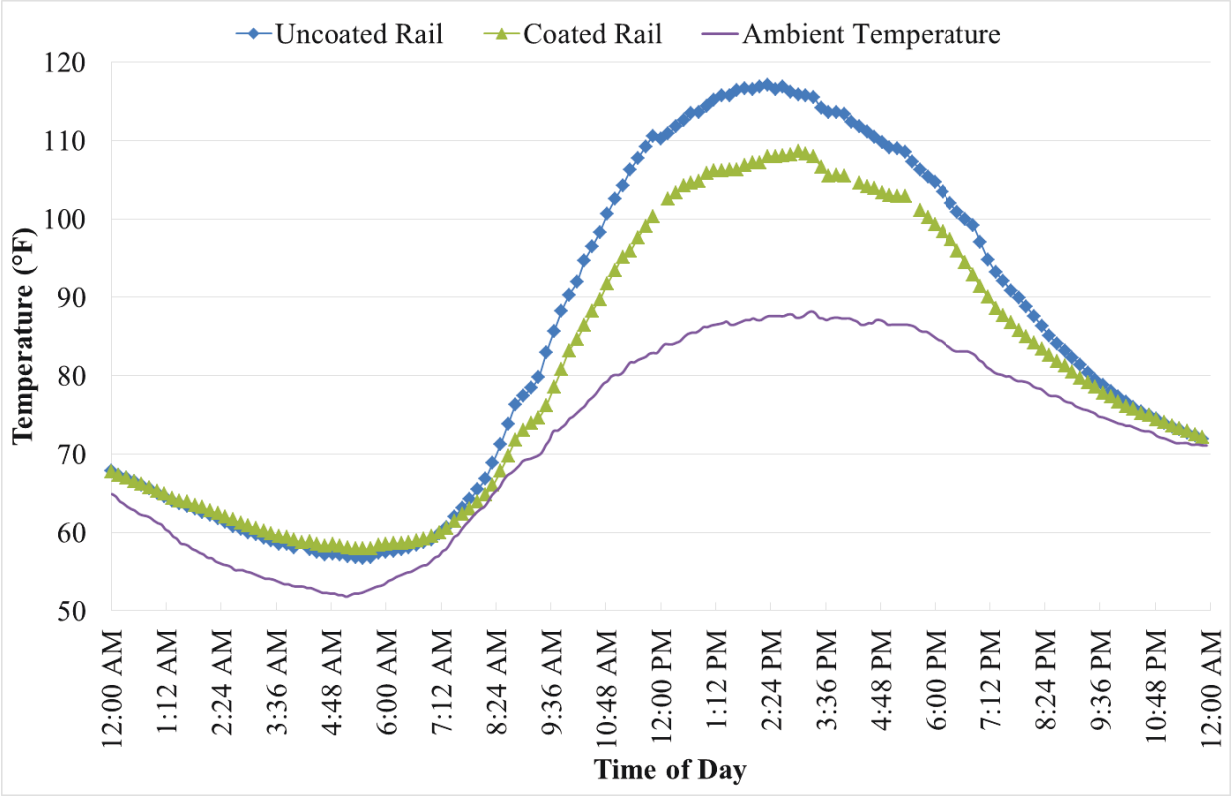

Figure 25. Example of Temperature Measurements at the NS Site (May 25, 2015)

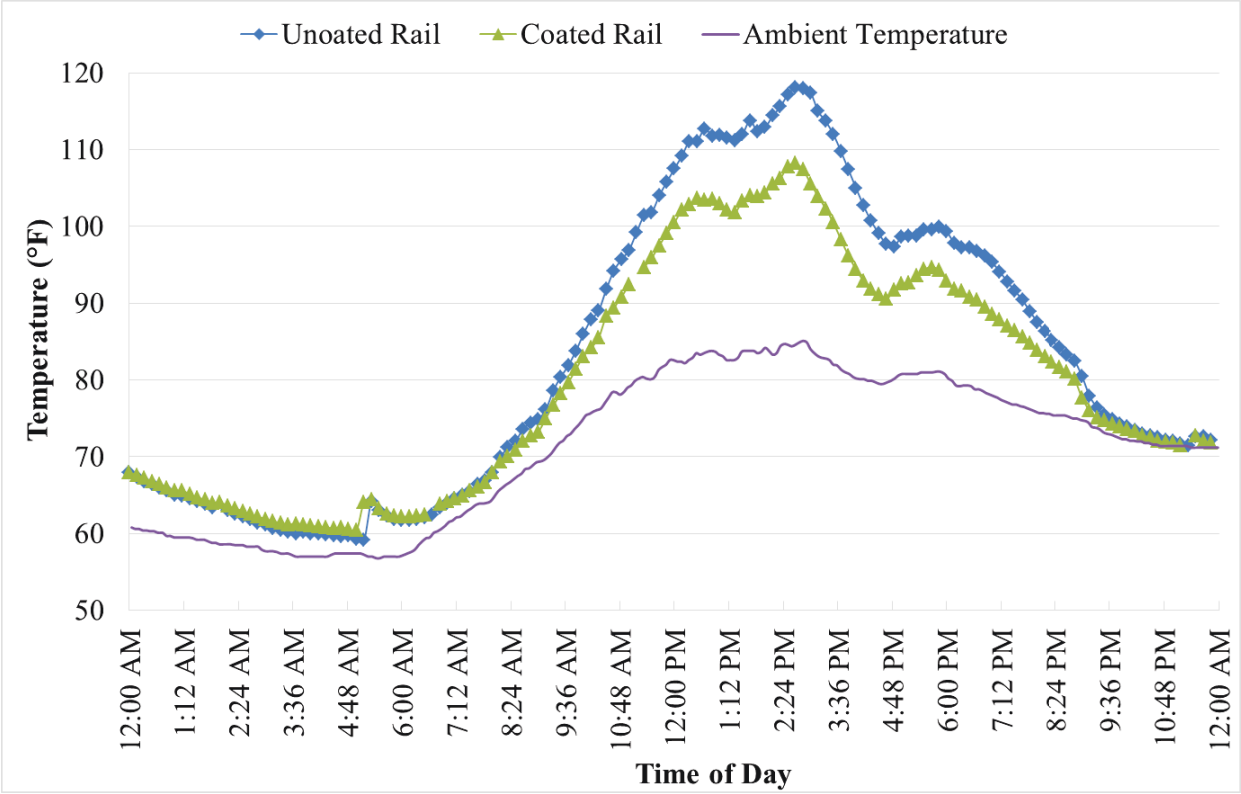

Figure 26. Example of Temperature Measurements at the NS Site (June 30, 2015)

Table 3 to Table 6 summarize the maximum reduction in temperature measurements at different days of each month in summer 2015. The highest rail temperature reduction due to coating was observed around 13 ºF and the range of temperature reduction varies between 8–13 ºF. The effect of coating on solar absorption appears slightly more effective in June, most likely due to the more intensive solar radiation in that month.

Table 3. Temperature Measurements from the NS Site (May 2015)

Date	Peak ambient temperature (°F)	Temperature of un-coated rail (°F)	Temperature of coated rail (°F)	Temperature reduction due to coating (°F)
5/23/15	70	88.5	78.7	9.8
5/24/15	82	94.2	85.3	8.9
5/25/15	87	106.2	95.9	10.3
5/26/15	89	105.9	96.7	9.2
5/27/15	89	111.4	102.1	9.3
5/28/15	89	115.3	105.1	10.2
5/30/15	88	110.7	101	9.7
Average	85	104.6	95.0	9.6

Table 4. Temperature Measurements from the NS Site (June 2015)

Date	Peak ambient temperature (°F)	Temperature of un-coated rail (°F)	Temperature of coated rail (°F)	Temperature reduction due to coating (°F)
6/7/15	78	97.5	84.3	13.2
6/8/15	84	107.7	96.8	10.9
6/11/15	91	108.8	99.4	9.4
6/16/15	84	99.8	89.5	10.3
6/30/15	82	117.4	105.6	11.8
Average	84	106.2	95.1	11.1

Table 5. Temperature Measurements from the NS Site (July 2015)

Date	Peak ambient temperature (°F)	Temperature of un-coated rail (°F)	Temperature of coated rail (°F)	Temperature reduction due to coating (°F)
7/6/15	84	117.5	108.7	8.8
7/16/15	81	103.5	94.8	8.7
7/17/15	82	112	103.8	8.2
7/25/15	89	107.7	98.9	8.8
7/30/15	88	110.5	102	8.5
Average	85	110.2	101.6	8.6

Table 6. Temperature Measurements from the NS Site (August 2015)

Date	Peak ambient temperature (°F)	Temperature of un-coated rail (°F)	Temperature of coated rail (°F)	Temperature reduction due to coating (°F)
8/2/15	89	105	96.3	8.7
8/11/15	81	101.9	92	9.9
8/20/15	89	95.2	86.4	8.8
8/24/15	86	118.5	109.7	8.8
Average	86	105.2	96.1	9.1

The data presented indicates discrepancies between the temperature reductions in the field-coated rail as compared to the results obtained from the outdoor lab experiment. One big difference is the instrumentation and temperature measurement method used in the experiments. The wired thermocouples in the outdoor experiment were glued to the rail by epoxy, while the thermal monitor with blue metal cover was used in the field experiment at the NS site.

It is believed that the blue metal cover of thermal monitor may cause additional variations in the temperature measurement. The thermal monitor may underestimate the temperature in the uncoated rail due to the color difference between blue cover and black uncoated rail, but overestimate the temperature in the coated rail due to the metal attachment in the coated rail. This effect may become more significant for the temperature measurements on the coated rail due to the big difference between the solar absorption coefficients of blue and white color. These effects were further investigated and discussed in Section 6.

5.4 Durability

The durability of the coating was evaluated by observing the performance of coated rails in the field subject to the weather conditions in New Jersey. The coated rails at the NS site were exposed to one summer cycle. All the coatings performed well even though there was rain

during the application at the NS site. These results confirm the results of laboratory experiments conducted in our previous studies in which the coating performed well when subjected to wetting and drying. Note that freeze-thaw cycles during winter in the field condition may induce more deterioration as compared to wetting and drying cycles conducted in the laboratory [29].

Field observations were conducted in December 2015 and April 2016, as shown in Figure 27 and Figure 28. The coating adhered well to the rail and no de-bonding or coating deterioration was observed after the summer and winter seasons.

(a)

(b)

Figure 27. Field Observation of Coated Rail on December 11, 2015

(a)

(b)

Figure 28. Field Observation of Coated Rail on April 20, 2016

6. Effects of Measurement Method on Rail Temperature

The effect of measurement method on rail temperature was investigated. The hypothesis is that the rail temperature is sensitive to the change of thermal properties such as solar absorption coefficient and thermal conductivity in the rail surface. This has been proven by the fact that the rail surface temperature decreases after the application of coating. The L.B. Foster Salient Systems temperature sensor was installed on rail surface with a large blue metal cover, which may affect the localized temperature condition. Therefore, additional experimental measurements and numerical simulations were conducted to evaluate the effect of thermal instrumentation on temperature measurements.

In June 2015, additional temperature measurements were made on the uncoated rail using rail thermometers (owned by NS) and a non-contact temperature gun. An average temperature value was obtained using 25 measurements at various ambient temperatures. The measurement data showed that the temperature measured by rail thermometer and temperature gun was higher than the temperature measured by the Salient system by an average value of 5 ºF. This is probably because the mounting style of the Salient system may affect the temperature measurement due to its heat "sink" effect. To account for the differences, the readings on the uncoated rail recorded using the Salient system should be adjusted to a higher value. Ideally, the NS site should be instrumented with the same thermocouple sensors used in the outdoor laboratory test (Section 4). Unfortunately, the research team did not have access to the rails to make this change.

In September 2015, temperature measurements were conducted on the coated rail using the wired thermocouples and the magnetic thermal sensors (K-type, purchased from Omega) in the outdoor laboratory testing. The hypothesis is that the metal magnet is attached to the rail for temperature measurement, so the magnet heats up and the temperature measurement for the area covered by the magnet could be affected.

Figure 29 and Figure 30 show the temperature measurements on two different days using the wired thermocouple and the magnetic thermal sensor. The results show that the rail temperatures measured using the magnet attachments were about 5 ºF to 8 ºF higher than the temperatures measured using thermocouples directly glued to the rails.

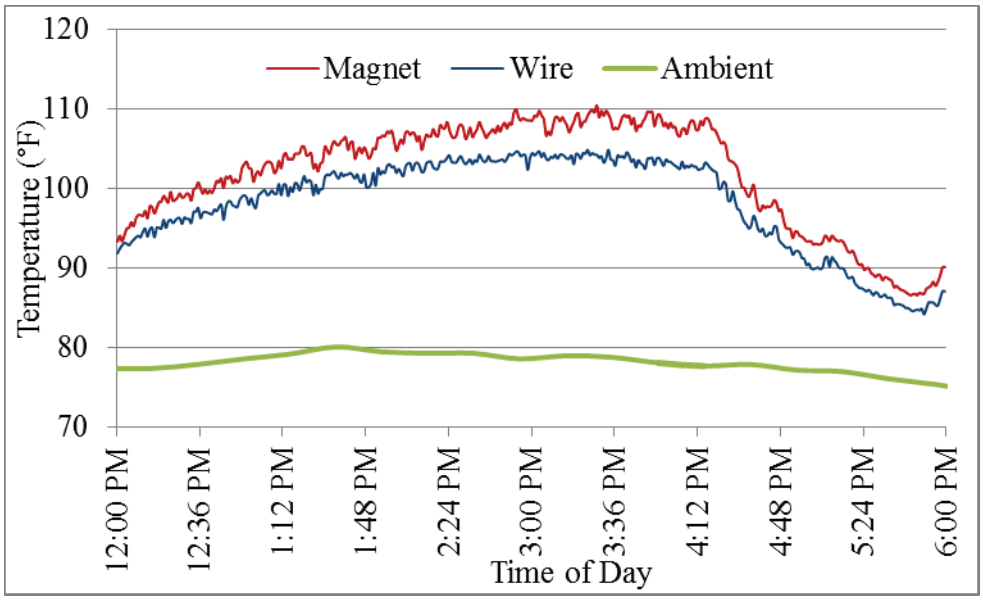

Figure 29. Difference in Rail Temperature Measured Using Magnet Sensor and Wired Thermocouple (Ambient Temperature at 80 ºF)

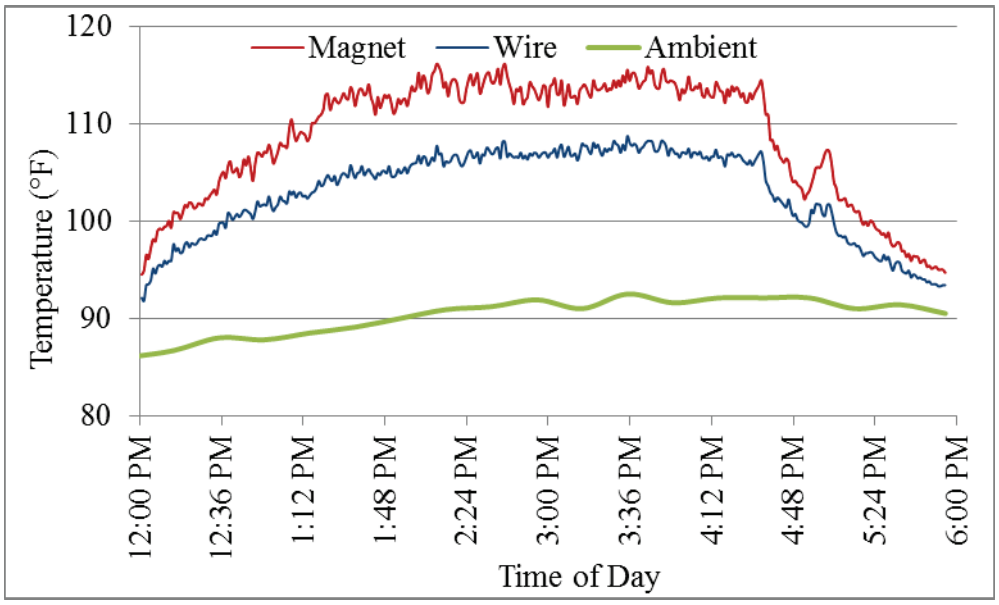

Figure 30. Difference in Rail Temperature Measured Using Magnet Sensor and Wired Thermocouple (Ambient Temperature at 92.5 ºF)

To further investigate if the change of solar absorption at the small area of rail surface (such as the metal cover in the temperature sensor) affects the rail temperature, thermal simulations were conducted using FE models. In the simulations, a 30-meter uncoated rail section was exposed to the diurnal solar radiation, wind velocity, and humidity. The weather data were obtained from the weather station in the outdoor laboratory testing as described in Section 4. A small segment of rail surface was assumed to have a different solar absorption coefficient from the original rail surface to simulate the metal cover effect due to thermal sensors, as shown in Figure 31. The

segment length (L) was varied from 0.1 m to 1 m. The metal cover was assumed to have blue color and thus much different solar absorption coefficient as compared to the uncoated (black) rail surface.

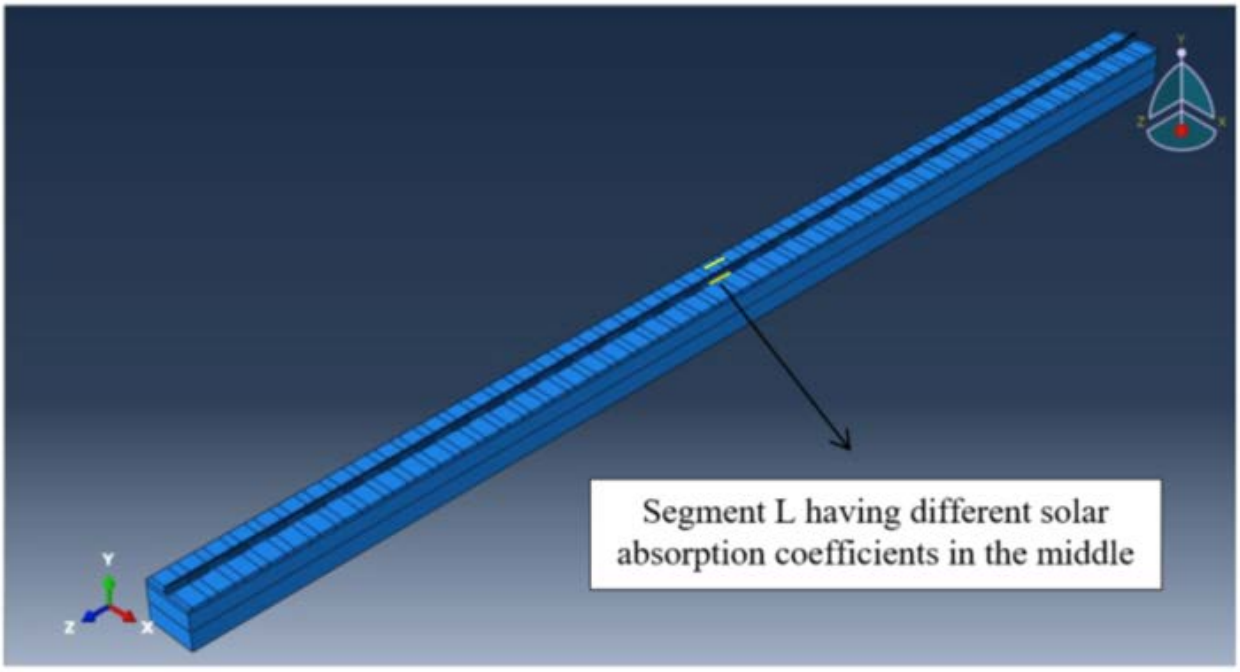

Figure 31. Illustration of Rail Section for Thermal Simulation

Figure 32 shows the simulated peak rail temperature at the center of segment where a smaller solar absorption coefficient was assumed. The temperature simulation results support the hypothesis that the rail temperature at localized area is sensitive to the change of solar absorption coefficient of rail surface that could be caused by the metal cover in the temperature sensor. For example, the temperature decreased by 5 ºF when the segment length was 0.2 m and the temperature reduction reached 10 ºF when the segment length increased to 0.8 m. This indicates that the attached blue cover of Salient system in the middle of uncoated rail may underestimate the temperature of the uncoated rail surface in the field section.

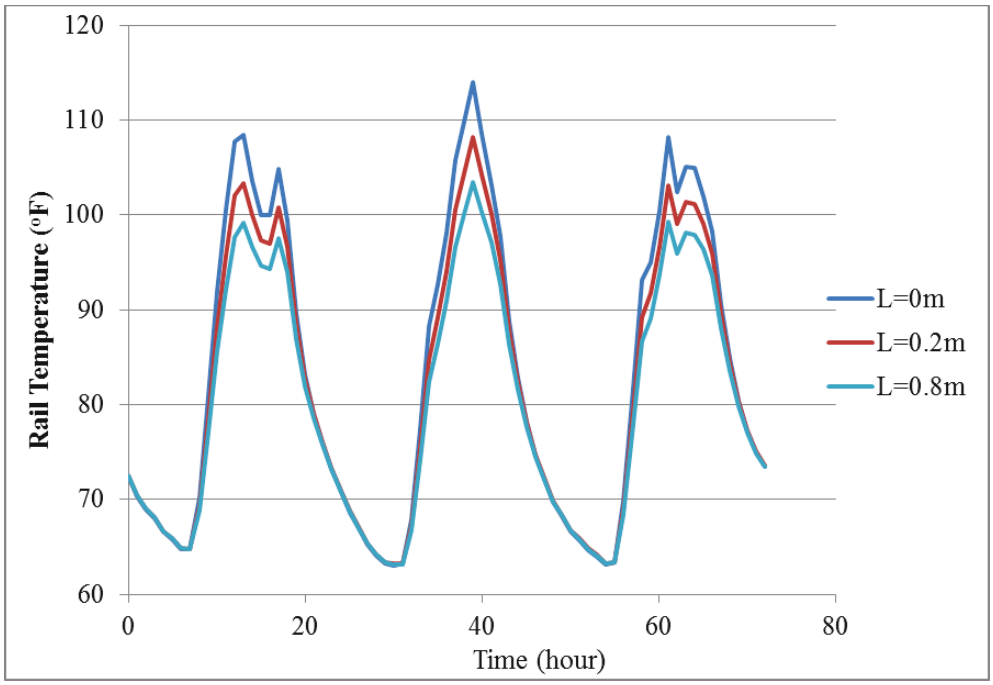

Figure 32. Variation of Rail Surface Temperature for Different Segment Lengths (L) (the Segment has the Smaller Solar Absorption than the Uncoated Rail Surface)

If the effect of the metal attachment with blue cover on temperature measurements is considered, the uncoated and coated rail temperatures measured with the Salient system need to be corrected in different ways. Based on the data presented above, this correction would cause the temperature difference between the uncoated and coated rail to approach 20 ºF, which is consistent with the observation from the earlier outdoor measurement using the wired thermocouples.

Table 7 contains the average temperature reduction values measured for each month after correction for potential errors using the measurement data obtained at the NS site.

Table 7. Effectiveness of Coating on Rail Peak Temperature After Correction of Potential Error Using the Measurement Data Obtained at the NS Site

Month	Corrected temperature of un-coated rail (°F)	Corrected temperature of coated rail (°F)	Temperature reduction due to coating (°F)
5/2015	109.6	90.0	19.6
6/2015	111.2	90.1	21.1
7/2015	115.2	96.6	18.6
8/2015	110.2	91.1	19.1
Average	111.6	92.0	19.6

7. Finite Element Simulation

This section describes the use of FE simulation to determine the effect of the measurement system on the measured rail temperature

7.1 Basic Theory of Heat Transfer

Three heat transfer modes were considered in the simulation of rail temperature: convection, radiation, and conduction. Heat flux exchanged through convection can be expressed by Eq. (1):

$$q_c = B \cdot (T_s - T_a) \tag{1}$$

Where, q_c is heat flux exchanged through convection, $W \cdot m^{-2}$; B is convective heat exchange coefficient, $W \bullet m^{-2} \bullet K^{-1}$. T_s and T_a are structure surface and air temperature respectively, K.

Solar radiation is the primary heating source for rail, and the rail emits radiation to the external environment. Thermal radiation between the rail surface and the natural environment mainly includes solar radiation, atmospheric radiation and structure surface radiation. The solar radiation comes from the sun and is influenced by the weather. The atmospheric radiation and structure surface radiation can be expressed as Eq. (2) and Eq. (3) respectively.

$$q_a = \varepsilon_a \sigma T_a^4 \tag{2}$$

$$q_r = \varepsilon_r \sigma T_s^4 \tag{3}$$

Where, q_a and q_r are atmospheric and structure surface radiation intensity respectively, $W \cdot m^{-2}$; ε_a is the atmosphere emissivity; ε_r is the structure surface emissivity; σ is Stefan–Boltzman constant $5.68 \times 10^{-8} W \cdot m^{-2} K^{-4}$; T_a is the air temperature, K; T_s is the structure surface temperature, K.

Conduction heat transfer happens inside the rail structure and between the rail and concrete sleepers. The governing equation can be expressed as Eq. (4):

$$\frac{\rho c}{k}\frac{\partial T}{\partial t} = \frac{\partial^2 T}{\partial x^2} + \frac{\partial^2 T}{\partial y^2} + \frac{\partial^2 T}{\partial z^2} \tag{4}$$

Where, T is temperature of structure, K; x, y and z are coordinates, m; ρ is density of material, kg/m^3; c is specific heat capacity, $J \bullet kg^{-1} \bullet K^{-1}$; k is thermal conductivity, $J \bullet m^{-1} \bullet s^{-1} \bullet K^{-1}$; and t is time, s.

Figure 33 illustrates the heat transfer between the rail and the surrounding environment.

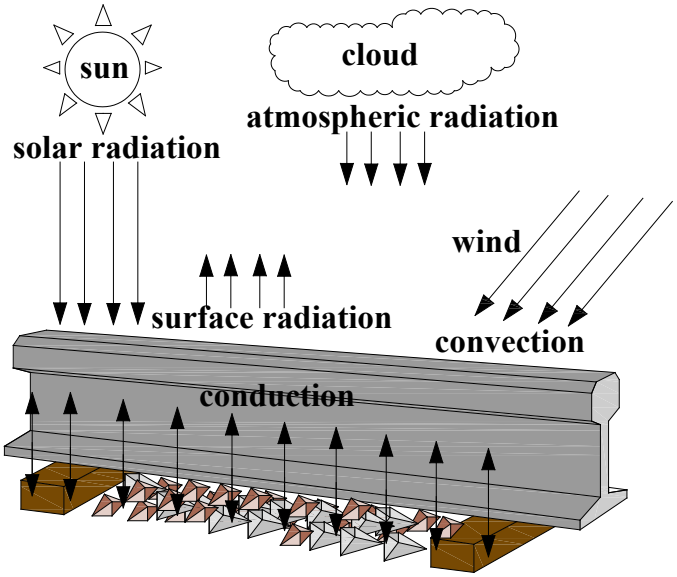

Figure 33. Heat Transfer Mechanism in Rail Temperature Field

7.2 Finite Element Model

Compared with field temperature prediction models in other fields such as highway pavement, there are very few rail temperature prediction models. Zhang and Al-Nazer established a rail temperature prediction model based on conservation of energy [8]. This model provided good results and was verified by comparing the model predictions to measured rail temperatures. Statistical regression is another effective method to build a rail temperature prediction model. The relationship between air temperature and rail temperature was analyzed by some researchers, such as Girardi et al. [9].

Current rail temperature prediction models provide reasonable results, but there are still some aspects that can be improved. In particular, the heat exchange between rail and base structure, such as sleepers and ballast, is neglected in these models. In addition, most current models are lumped parameter models. The temperature difference inside the rail is neglected. In other words, most current rail temperature models focus on the average rail temperature, but not the temperature profile distribution in the cross-section of rail. This may cause some error in prediction of peak rail temperature and any subsequent thermal stress.

The research team at Rutgers developed a 3D FE heat transfer model to simulate the temperature fields within rail segments in the outdoor experiment. The FE model employed ABAQUS commercial FE software. The rail segment was placed on a concrete slab above a deep soil layer. The total depth of the concrete layer and soil layer was big enough in the model to ensure the insulation condition at the bottom of soil layer. The detailed dimensions of the 3D FE heat transfer model are shown in Figure 34.

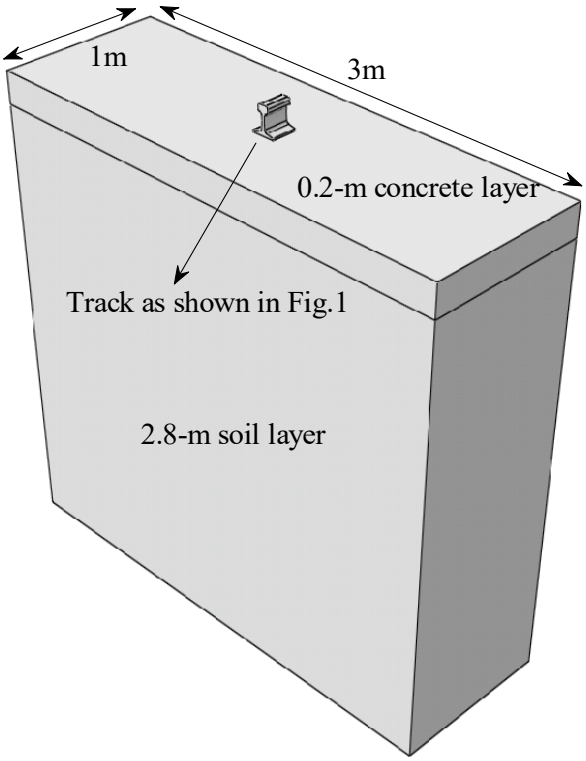

Figure 34. Dimensions of 3D FE Heat Transfer Model

Material properties used in the heat transfer model and the subsequent thermal stress analysis are shown in Table 8. Air temperature, solar radiation and wind speed are three important climatic factors related to heat transfer between rail structure and the external environment. These factors were obtained from the outdoor experiment and used in the FE simulation.

Table 8. Material Properties Used in Finite Element Modeling [30–38]

Material	Uncoated steel	Coated steel	Concrete	Ballast	Soil
Density/kg•m^{-3}	7801	7801	2270	2190	1782
Thermal conductivity /J•m^{-1}•s^{-1}•℃$^{-1}$	43	43	0.8	1.1	0.8
Specific heat/J•kg^{-1}•℃$^{-1}$	473	473	883	1000	1040
absorptivity	0.75	Back calculate	0.6	0.55	Not needed
emissivity	0.75	0.75	0.85	0.45	Not needed
Elastic modulus/ MPa	200000	200000	72400	250	330
Poisson's ratio	0.3	0.3	0.33	0.4	0.25
Thermal expansion coefficient/ 10^{-5}℃$^{-1}$	1.15	1.15	9.8	Not needed	Not needed

7.3 Temperature Prediction

The air temperature, solar radiation, and wind speed recorded during the experiment are shown in Figure 35 to Figure 37. The air temperature shows the diurnal variation between days and nights, while the solar radiation may vary in the daytime depending on the cloud cover. The recorded highest air temperature is 30.4 °C (86.7 ºF). The wind speed is in general small within the range of 1–2mph.

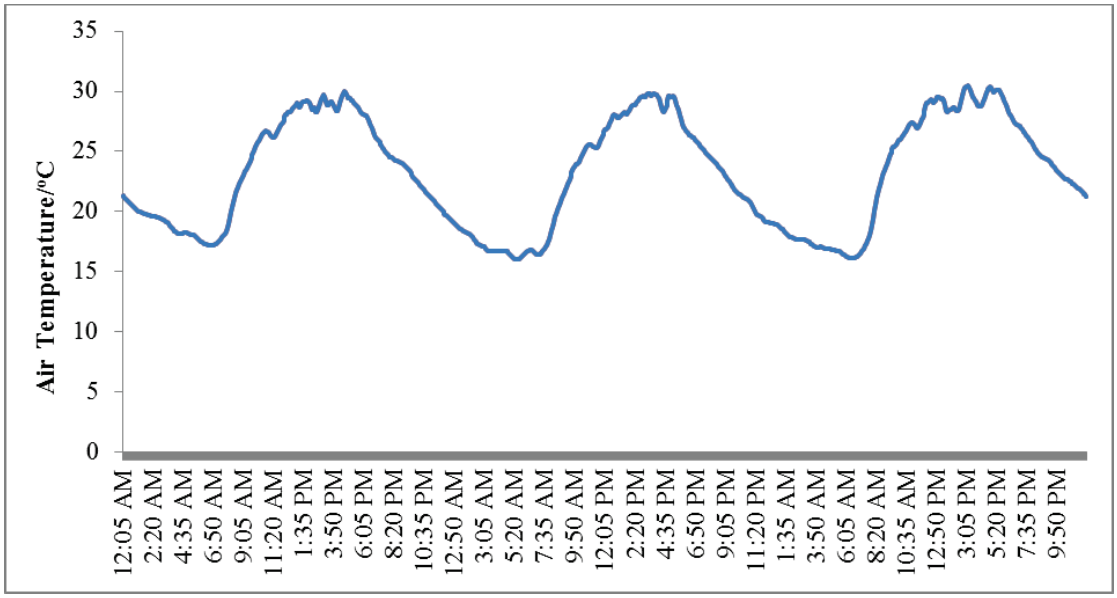

Figure 35. Air Temperature During the Experiment (August 7–9, 2014)

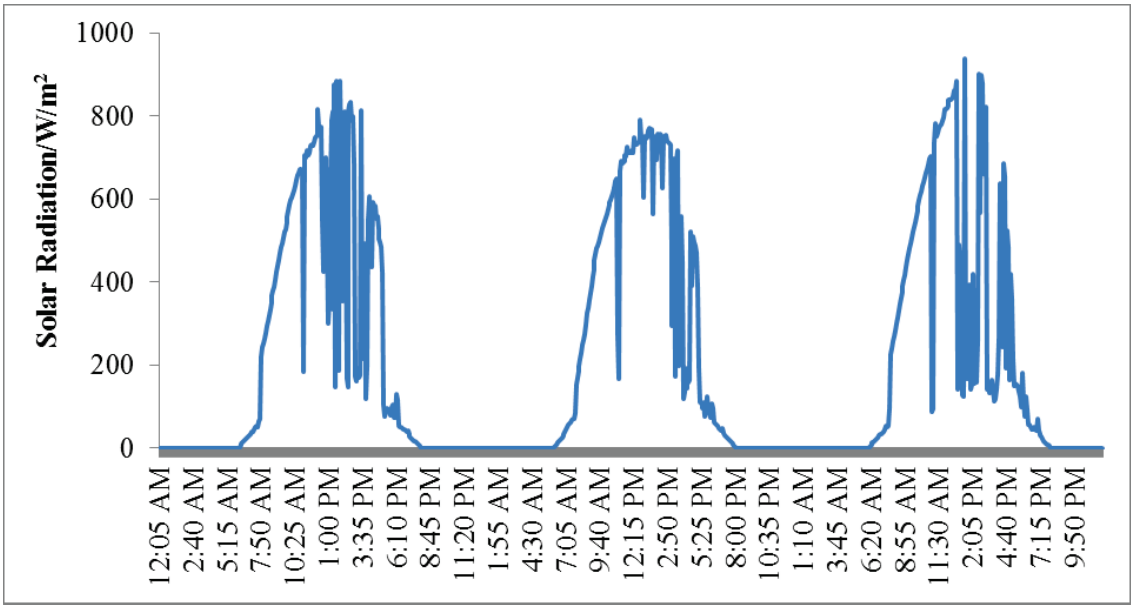

Figure 36. Solar Radiation During the Experiment (August 7–9, 2014)

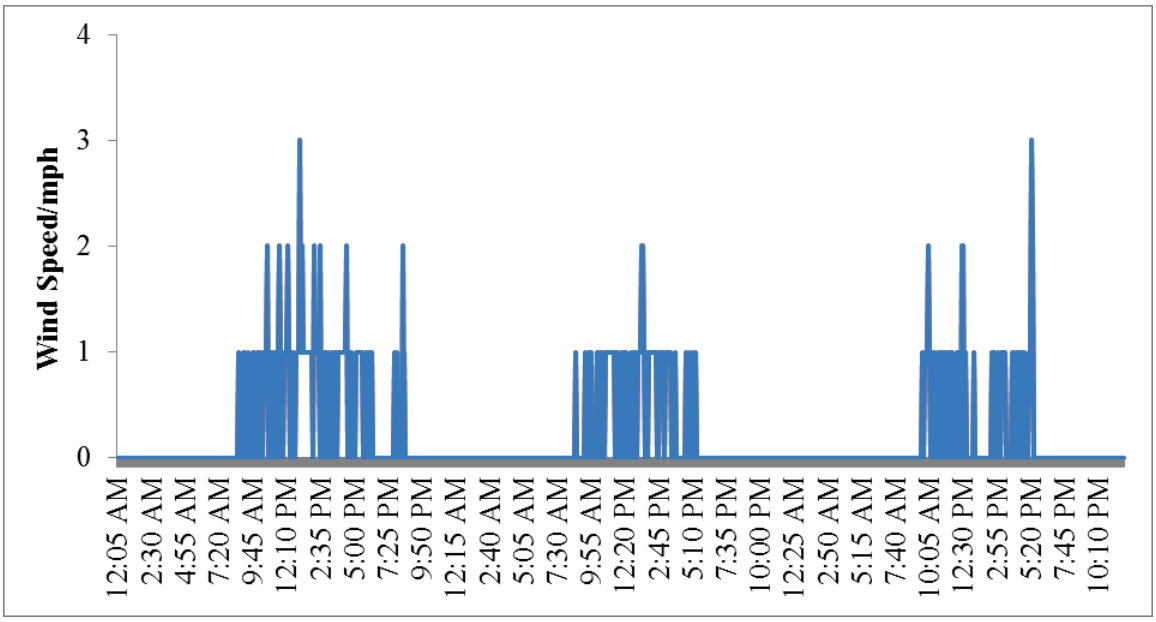

Figure 37. Wind Speed During the Experiment (August 7–9, 2014)

The temperature data of the coated and uncoated rail segments during the outdoor laboratory experiment are shown in Figure 38. The data shows that the coating significantly decreases the rail peak temperature, especially the highest daily temperature. The largest reduction in rail temperature was around 10.5 °C (19 ºF). On the other hand, the coating did not affect the lowest daily temperature. This trend is consistent with the temperature observation from the outdoor laboratory testing as described in Section 4.

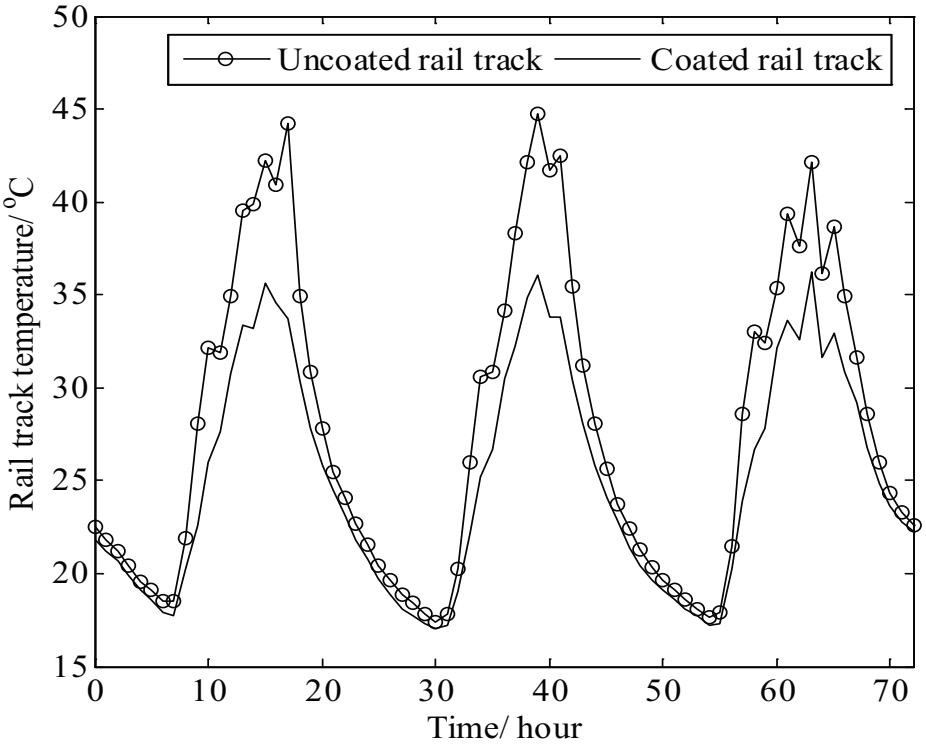

Figure 38. Temperature of Coated and Uncoated Rail Segments (August 7–9, 2014)

The temperature field of the uncoated rail segment was first predicted using the developed FE model. The comparison between the predicted and measured values at the location of the rail web where the temperature sensor was placed is shown in Figure 39. The results show that the predicted results from the FE model compare well with the experiment data. The average relative error between the predicted and measured temperatures is 4.4 percent.

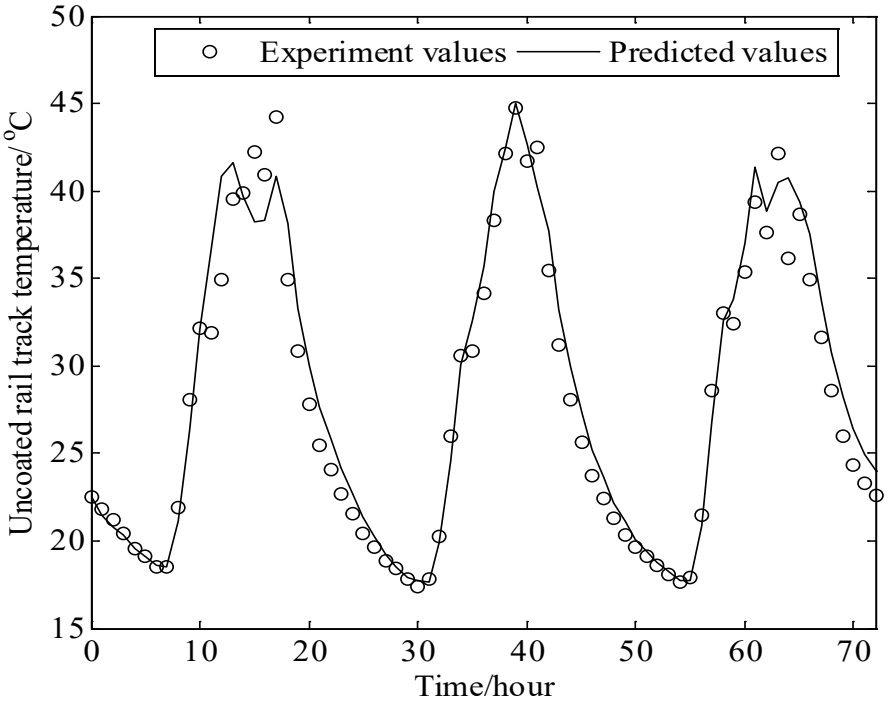

Figure 39. Comparison Between Predicted and Measured Uncoated Rail Temperatures

7.4 Solar Absorptivity of Coating

The solar radiation absorbed by rail is related to solar absorptivity, while the radiation emitted from rail is related to emissivity. The cooling mechanism of the coating reduces the level of solar absorptivity of rail. The solar absorptivity of coating is affected by the purity of while color and chemical compositions of coating material. The 3D FE model was used to back calculate the solar absorptivity of the coated rail based on experimental measurements.

To achieve this purpose, rail temperatures were calculated using different values of solar absorptivity, ranging from 0.75 (initial value) to zero. The calculated rail temperatures were compared to experiment measurements. The average relative errors using different values of solar absorptivity were calculated, as shown in Figure 40. The minimum average relative error was obtained when the solar absorptivity was equal to 0.2. Therefore, the solar absorptivity of coating in the experiment was determined as 0.2. This result is consistent with the typical absorptivity values estimated from the chemical compositions of coating material.

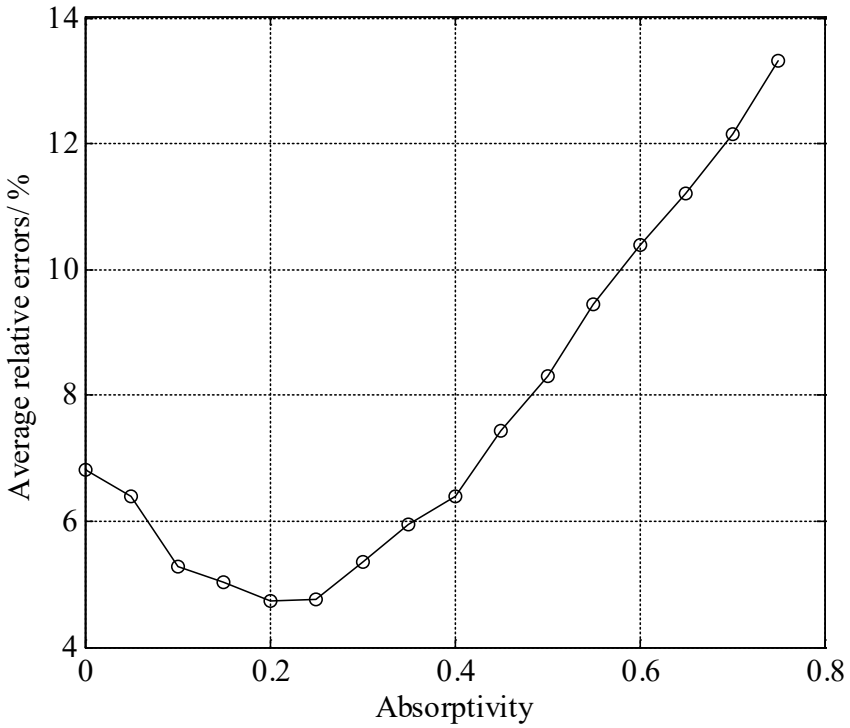

Figure 40. Variation of Average Temperature Errors with Coating Solar Absorptivity

To validate the back calculated solar absorptivity of the coating, the absorptivity value (0.2) was used to predict the coated rail temperatures at different ambient environmental conditions. The average errors, largest errors, average relative errors, and largest relative errors between experiment measurements and prediction results are shown in Table 9. The results show that although the average relative errors in the validation cases were higher than the smallest one shown in Figure 40, the experiment data and the predicted values were close in general for all validation cases. In particular, the peak temperature error was smaller than 2.2 °C (3.96 ºF). This validates that the back-calculated solar absorptivity of the coating was reasonable for temperature prediction of coated rail.

Table 9. Errors Between Measured and Predicted Temperatures

Date	Average errors/°C	Errors at peak temperature/°C	Average relative errors/ %	Relative errors at peak temperature /%
6/1/2014	2.2	0.8	7.7	2.4
6/20/2014	1.3	0.2	5.1	0.7
6/28/2014	2.5	2.2	7.5	5.8

7.5 Calculation of Thermal Stress

A 3D FE model was developed to study the effect of low solar absorption coating on thermal stresses caused by daily temperature variations in the rail. In the FE model, one 5-ft American Railway Engineering and Maintenance-of-Way Association (AREMA) rail (119 lb/yd) was

placed on three concrete ties. The length, width, and depth of the concrete ties were 2.7432 m, 0.2286 m, and 0.1178 m, respectively. A 0.45-m ballast layer and a 0.5-m soil foundation layer were placed under the concrete sleeper. Full bonding condition was considered for the contact between rail and concrete sleepers that did not allow any slippage movement at the contact interface. To reduce computation time, symmetric conditions were used. The dimensions of the FE model are shown in Figure 41.

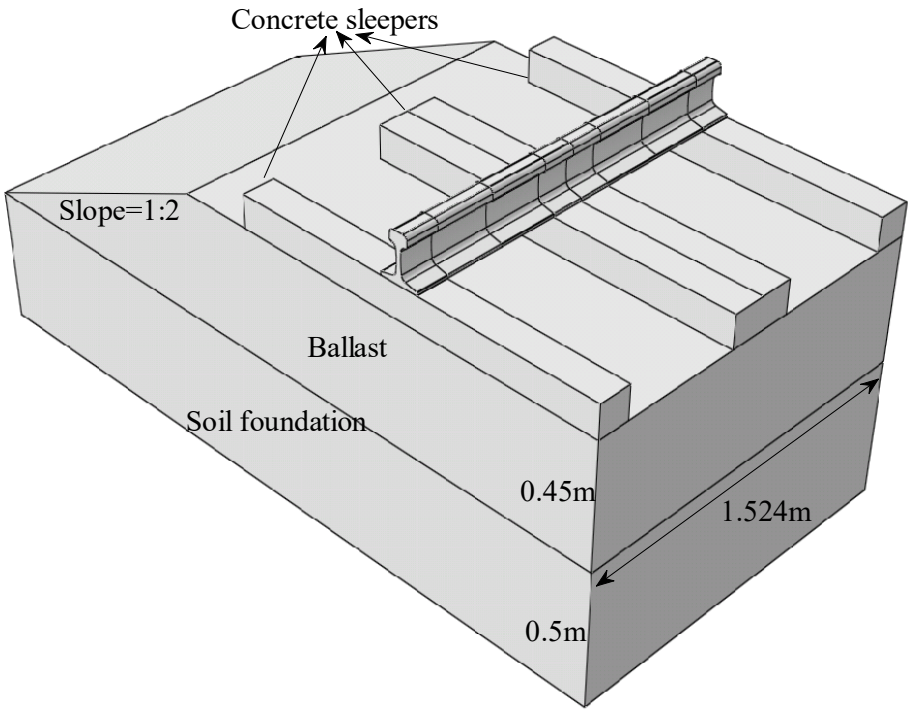

Figure 41. Dimensions of 3D FE Thermal Stress Model

With the climatic factors (Figure 35, Figure 36, and Figure 37) and material properties (Table 8) shown above, temperature fields and thermal stresses in the rail were simulated. For the hottest hour, the temperature contours at the center of the rail are shown in Figure 42 for the uncoated rail and Figure 43 for the coated rail. The results show the temperature distributions inside the rail are not uniform. In the uncoated rail, the maximum temperature difference within the rail was up to 2.5 °C (4.5 ºF). The non-uniform temperature distribution was mainly caused by the variation of thermal boundary conditions at ballast and concrete sleeper.

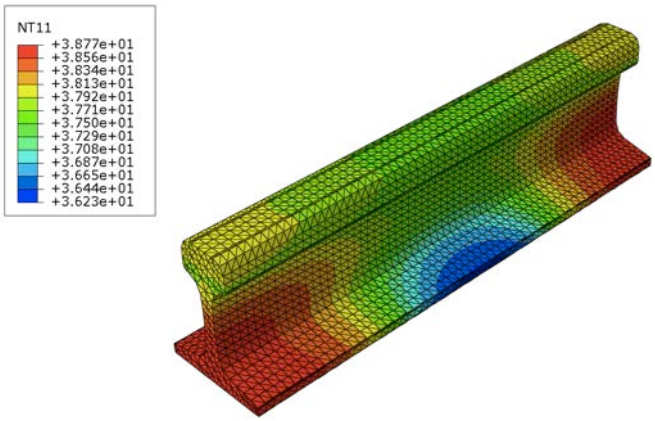

Figure 42. Temperature Contour of the Uncoated Rail (the Highest Temperature is 38.77 °C)

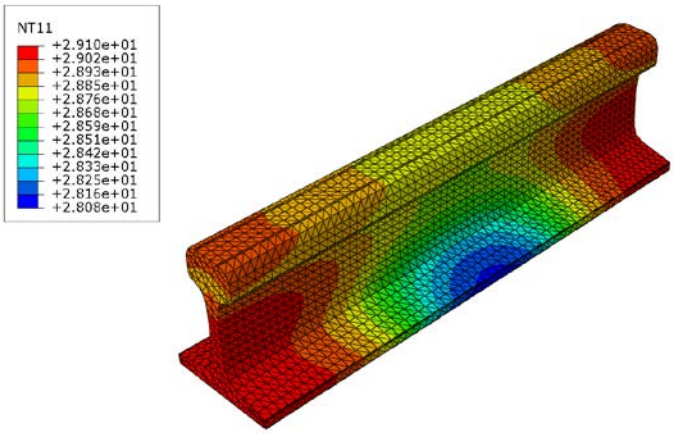

Figure 43. Temperature Contour (ºC) of the Coated Rail (the Highest Temperature is 29.10 °C)

An earlier study by Amtrak showed that the rail neutral temperature (RNT) reduced after installation due to traffic and maintenance, as shown in Figure 44 [6]. The lowest and average RNT were about 18 and 38 °C (64 and 100 ºF) respectively from field measurements between Philadelphia and Washington. These two RNT cases were used in this study to calculate the possible thermal stress in the rail due to daily temperature variations. The predicted longitudinal thermal stresses are shown in Figure 45.

The results show that, when the RNT was low (18 °C [64 ºF]), compressive thermal stresses were present nearly every day. In this case, significant compressive stresses were observed in the uncoated rail during the hot hours. With the low absorptivity coating, the compressive thermal stresses were significantly decreased, up to about 50 percent at the hottest hours. This indicates that the coating application could significantly reduce rail buckling risk on hot days. On the other hand, when the RNT is high (38 °C [100 ºF]), the compressive thermal stresses in the uncoated track during hot hours were very small. This was because the ambient temperature was usually lower than the rail's neutral temperature. However, tensile stresses were observed in

the rail during cool hours, which indicates a risk of rail break. In this case, the low solar absorption coating decreases the daily fluctuation of rail thermal stress, which may reduce thermal fatigue in rail.

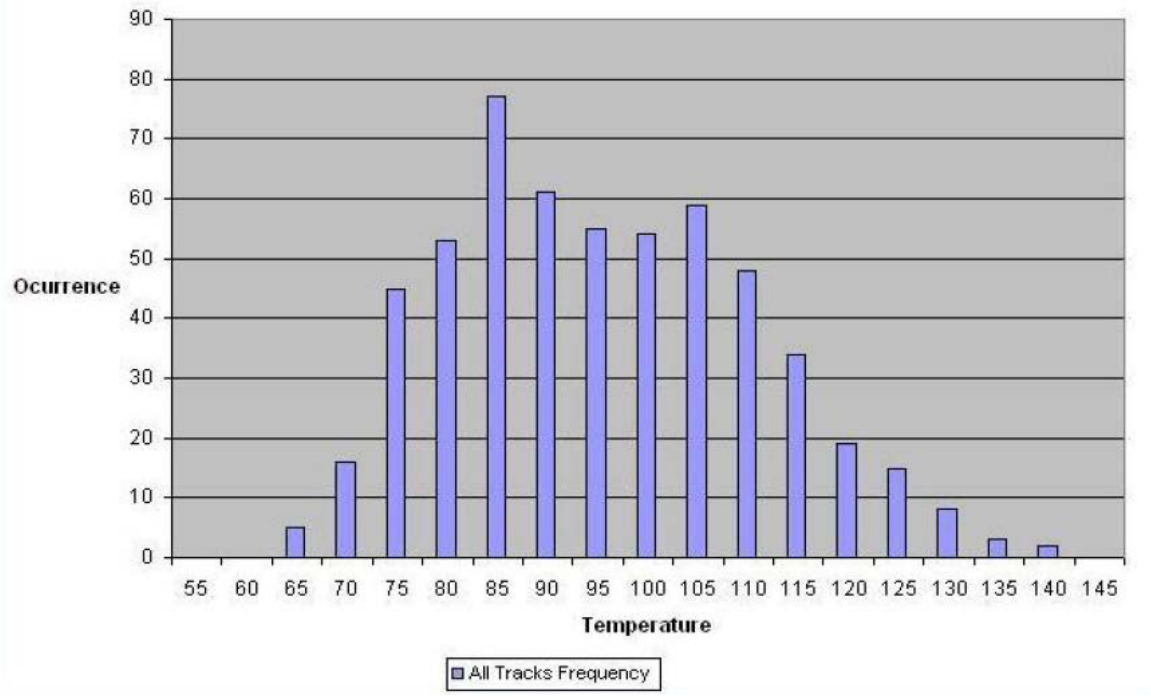

Figure 44. Distribution of Rail Neutral Temperature (°F) from Literature [6]

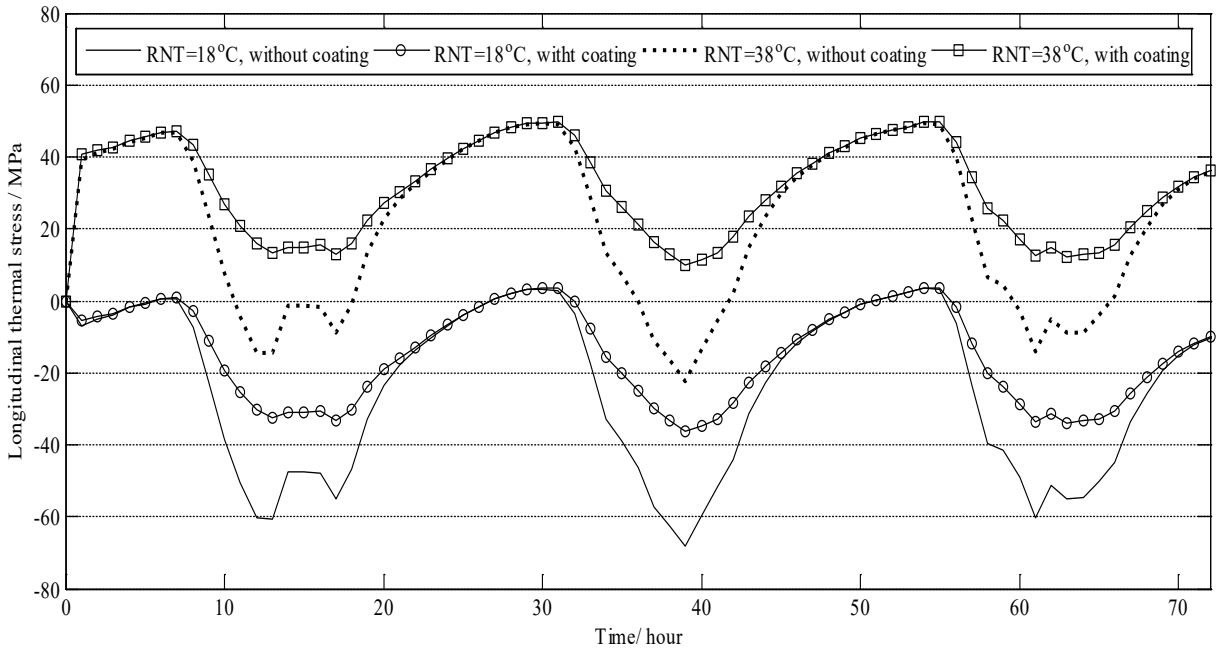

Figure 45. Longitudinal Thermal Stresses at the Centroid of Track (Negative: Compression, Positive: Tension)

In the railroad community, the RNT is usually set at a relatively high temperature to prevent bulking. For example, the Amtrak policy is to set the RNT in the range of 32 ° to 43 °C (89 to 109 ºF) during installation [28]. The coating application could reduce the high RNT requirement during rail placement. This would save rail operation cost and as well as reduce the risk of rail break due to tension. The track's longitudinal restraint capacity may be affected by traffic and maintenance, likely reducing RNT. In this case, the coating could reduce the risk of rail buckling due to compression. It is envisioned that the coatings would be applied at select locations that may have an increased probability of buckling. Therefore, the low solar absorption coating could serve as a proactive way to control peak temperatures and thermal stresses in the rail.

8. Conclusion

Researchers at Rutgers University successfully completed all tasks under the research projects. The research findings and recommendations for additional work are presented in this section.

8.1 Findings

In this study, a low solar absorption coating for rail application was developed to reduce the peak rail temperature and prevent rail buckling and derailments on hot days. The zero-volatile organic content (VOC) and 100 percent inorganic coating system was based on an alkali-aluminosilicate composite formulation.

The outdoor lab experiment results show that the maximum temperature reduction provided by the coating was 26 ºF with an average of 21 ºF. The rail temperature did not exceed 11 ºF above the ambient temperature for the coated rail. On average, the coating reduced the temperature gain by 66 percent. The results were consistent during the monitoring period lasting several months. The observations from this study are consistent with the results reported in another rail coating study using inorganic and organic coatings commercially available. Both studies show the superior performance of inorganic coating for low solar absorption.

It was discovered that the measurement of rail temperature is affected by the small area change of rail surface with different solar absorption coefficients such as the metal attachment in the magnetic temperature sensor. Considering these effects, the rail temperature measured with the automated system was corrected. This correction difference between the uncoated and coated rail in the field track is approximately 20 ºF, which is consistent with the observation from the outdoor lab measurement using the wired thermocouples.

Three-dimensional FE models were developed to predict temperature distributions and thermal stresses in the rail. The simulation shows that, when the rail neutral temperature (RNT) is low, the coating decreases the compressive thermal stresses up to about 50 percent during the hottest hours. Although increasing the RNT decreases compressive thermal stresses in the rail, it increases the risk of rail break. The coating application could reduce the high RNT requirement during rail placement and prevent rail buckling when the effective RNT decreases after traffic and maintenance.

Field application of coating demonstrates that the coating adheres well to the rails. Extensive surface preparation is not needed and pressure washing with water is sufficient. Coating can be applied using regular equipment such as brush or rollers. Since the curing time for allowing rail-traffic is about an hour, the coating can be applied on active tracks with proper scheduling. The durability of the coating was observed over summer and winter seasons and the coating performed well.

8.2 Future Research Recommendation

For the coating materials, white or off-white color will be used in upcoming FRA research as it provides least solar absorption in the visible spectrum of sunlight. The coating formulation can be further improved by adding nano-particles to reflect near-infrared radiation for low solar absorption.

Benefit-cost analysis should be conducted for the rail coating system considering material cost, application cost and possible maintenance cost.

Future research is recommended to monitor the long-term behavior of coated rail as compared to that of uncoated rail in terms of temperature reduction and durability of coating.

9. References

1. Federal Railway Administration's Office of Safety Analysis. (2012). Fiscal Year 2012 Accident/Incident Overview. Available at: http://safetydata.fra.dot.gov/OfficeofSafety/publicsite/Query/AccidentByRegionStateCounty.aspx.
2. Bruzek, R., Biess, L., and Al-Nazer, L. (2013). "Development of Rail Temperature Predictions to Minimize risk of Track Buckle Derailments." 2013 Joint Rail Conference: Knoxville, TN.
3. Barkan, C., Dick, Tyler, P. L., C., and Robert, A. (2003). "Railroad Derailment Factors Affecting Hazardous Materials Transportation Risk." Transportation Research Record: Journal of the Transportation Research Board, *1825*, 64–74.
4. Liu, X., Rapik Saat, M., and Barkan, C. P. L. (2012). "Analysis of Causes of Major Train Derailment and Their Effect on Accident Rates." Transportation Research Record: *Journal of the Transportation Research Board*, *2289*, 154–163.
5. Kish, A., Samavedam, G. (1999, December 2–3). "Risk Analysis Based CWR Track Buckling Safety Evaluations." Proceedings of International Conference on Innovations in the Design & Assessment of Railway Track: Delft University of Technology, the Netherlands.
6. Trosino, M., and Chrismer, S. (2009). "Changes in AMTRAK's Heat Order Policy," AREMA 2009 Annual Conference: Chicago, IL.
7. Bruzek, R., Biess, L., Kreisel, L., and Al-Nazer, L. (2014). Rail Temperature Prediction Model and Heat Slow Order Management. 2014 Joint Rail Conference: Colorado Springs, CO.
8. Zhang, Y. J., and Al-Nazer, L. (2010). "Rail Temperature Prediction for Track Buckling Warning." AREMA 2010 Annual Conference: Orlando, FL.
9. Girardi, L., Boulanger, D., Laurans, E., Pouligny, P., Xu, Y., and Colibri, J. (2011). "Rail Temperature Forecasts Over Different Time-Ranges for Track Applications." 5th IET Conference on Railway Condition Monitoring and Non-Destructive Testing: Derby, UK.
10. Uemoto, K.L., Neide, M. N. S., and Hohn, V. M. (2010). "Estimating Thermal Performance of Cool Colored Paints." *Energy Buildings*, *42*(1): 17–22.
11. Doulos, L., Santamouris, M., and Liviada, I. (2004). "Passive Cooling of Outdoor Urban Spaces, the Role of Materials." *Solar Energy*, *77*(2), 231–249.
12. Sunnefa, A., Santamouris, M., and Livada, I. (2006). "A Study of the Thermal Performance of Reflective Coatings for the Urban Environment." *Solar Energy*, *80*(8), 968–981.
13. Paintsquare Feds: (2013). *Heat Caused Fatal Bridge Collapse*. Available at: http://www.paintsquare.com/news/?fuseaction=view&id=9971.
14. Tran, N., Powell, B., Marks, H., West, R., and Kvasnak, A. (2009). "Strategies for Design and Construction of High-Reflectance Asphalt Pavements." Transportation Research Record, 2098, 124–130.

15. US DOT John A. Volpe Transportation Center. (2018). *Track Buckling Research*. Available at: https://www.volpe.dot.gov/infrastructure-systems-and-technology/structures-and-dynamics/track-buckling-research.

16. Kish, A., and Samavedam, G. (2013). "Track Buckling Prevention: Theory, Safety Concepts, and Applications." Technical Report, DOT/ FRA/ORD-13/16. Available at: https://www.fra.dot.gov/eLib/details/L04421.

17. Bendiganavale, A. K., and Malshe, V. C. (2008). "Infrared Reflective Inorganic Pigments," *Recent Patents on Chemical Engineering*, *1*, 67–79. Available at: http://busseiqanda.la.coocan.jp/Infrared_reflecting_pigment.pdf.

18. Holophane. (2017). *Paint Finishes and Prismatect*. Available at: http://www.holophane.com/education/tech_docs/jg2.pdf.

19. Solocoat. (2018). "Solacoat Heat Reflective Metal and Porous Roof Coating System." Available at: http://solacoat.com.au/Solacoat-Topcoat-pg26479.html.

20. MacDonald, R. D, Armstrong, M., and Fritz, B. (2001). Reducing Solar Heat Gain with Ceramic Coatings. Available at: http://www.protek-usa.com/pdf-new/reports/RDSHGwCC.pdf.

21. Elvin, G. (2007). Nanotechnology for Green Building, Green Technology Forum.

22. Millward, D. (2013). "Heat hits train punctuality: tracks to be painted white to counteract hot weather." Available at: http://www.telegraph.co.uk/news/uknews/road-and-rail-transport/10204211/Heat-hits-train-punctuality-tracks-to-be-painted-white-to-counteract-hot-weather.html.

23. Pacific Edge, Ltd. (2005, October). "Rail Painting Process." Available at: http://solacoat.com.au/rs/7/sites/1164/user_uploads/File/Reports/Solacoat%20Rail%20Painting%20Process.pdf.

24. Ritter, G. W., and Al-Nazer, L. (2014). "Coatings to Control Solar Heat Gain on Rails," AREMA 2014 Annual Conference: Chicago, IL.

25. Papakonstantinou, C. G., and Balaguru, P. N. (2007). "Fatigue Behavior of High Temperature Inorganic matrix composites." *Journal of Materials in Civil Engineering*: ASCE, *19*(4), 321–328.

26. Najm, H., Secaras, J., and Balaguru, P. N. (2007). "Compression Tests of Circular Timber Column Confined with Carbon Fibers Using Inorganic Matrix." *Journal of Materials in Civil Engineering*: ASCE, *19*(2), 198–204.

27. Toutanji, H. A., Zhao, L., Deng, Y., Zhang, Y., and Balaguru, P. N. (2006). "Cyclic Behavior of RC Beams Strengthened with Carbon Fiber Sheets Bonded by Inorganic Matrix." *Journal of Materials in Civil Engineering*: ASCE, *18*(1), 28–35.

28. Balaguru, P. N., Nanni, A., and Giancaspro, J. (2009). "FRP Composites for Reinforced and Prestressed Concrete Structures." New York: Taylor and Francis.

29. Balaguru, P. N., and Lee, K.W. (2001). "Effectiveness of High Strength Composites as Structrual and Protective Coating for Structural Elements." Final Report NETCR 28: New England Transportation Consortium.

30. Annaratone, D. (2010). Engineering Heat Transfer. Springer-Verlag Berlin Heidelberg.

31. Kesler, K., and Zhang, Y. J. (2007). System and Method for Predicting Future Rail Temperature. United State Patent NO: 2007/0265780A1.

32. The Engineering ToolBOX Emissivity Coefficients of Some Common Materials. Available at: https://www.engineeringtoolbox.com/emissivity-coefficients-d_447.html.

33. Hall, M. R., Dehdezi, P. K., Dawson, A. R., Grenfell, J., and Isola, R. (2012). "Influence of the Thermophysical Properties of Pavement Materials on the Evolution of Temperature Depth Profiles in Different Climatic Regions." *Journal of Materials in Civil Engineering*, *24*(1), 32–47.

34. Cote, J, and Konrad, J. M. (2005). Thermal Conductivity of Base-Course Materials, *Canadian Geotechnical Journal*, *42*(2), 443–458.

35. The Engineering ToolBOX. "Absorbed Solar Radiation." Available at: https://www.engineeringtoolbox.com/solar-radiation-absorbed-materials-d_1568.html.

36. Grissom, G. T., and Kerr, A. D. (2006). "Analysis of Lateral Track Buckling Using New Frame-Type Equations." *International Journal of Mechanical Sciences*, *48*(1), 21–32.

37. The Engineering ToolBOX. Coefficients of Linear Thermal Expansion. Available at: https://www.engineeringtoolbox.com/linear-expansion-coefficients-d_95.html.

38. Sadeghi J., and Askarinejad, H. (2010). "Development of Nonlinear Railway Track Model Applying Modified Plane Strain Technique." *Journal of Transportation Engineering*, *136*(12), 1068–1074.

Appendix A.
A Guideline for Coating Application

The following is the recommendations for specification and guidelines for application of coating.

The process consists of the following three steps.

Step 1: Clean the rails to remove dust, oil and other impurities from the surface. High pressure washing (2,500 psi) with water is sufficient.

Allow the surface to dry.

Step 2: Prepare the coating material and apply to the sides and bottom flange of the rails.

The inorganic-coating is supplied in two parts. Part A is a liquid and Part B is powder. Mix the two components using a high shear mixer. Regular drill in combination with paint mixer with a minimum of 1,500 rpm is sufficient.

Apply the coating using a roller or airless sprayer.

Step 3: Protect the surface from rain and other water sources for at least 3 hours.

Train traffic can be allowed after 1 hour.

Step 4: If needed, apply the second layer coating at 24 hours after application of the first layer.

Abbreviations and Acronyms

CWR	Continuous Welded Rail
FRA	Federal Railroad Administration
FTA	Federal Transit Administration
FE	Finite Element
NSW	New South Wales
NS	Norfolk Southern Corporation
RIC	RailCorp
RNT	Rail Neutral Temperature
3D	Three-Dimensional
VOC	Volatile Organic Content